농 학 석 사 학 위 논 문

애기장대 엽록체 발달에 관여하는 Plastid-Encoded RNA Polymerase-Associated Protein 3 단백질의 역할 규명

Characterization of Plastid-Encoded RNA Polymerase-Associated Protein 3 in Development of Chloroplast in *Arabidopsis*

2018년 8월

서울대학교 대학원
농생명공학부 응용생명화학전공
장 순 현

Abstract

Characterization of Plastid-Encoded RNA Polymerase-Associated Protein 3 in Development of Chloroplast in *Arabidopsis*

Sun Hyun Chang

Department of Agricultural Biotechnology
The Graduate School
Seoul National University

Plastid-encoded RNA polymerase (PEP) is essential for chloroplast development by controlling expression of plastid genes. Previous studies revealed that PEP activity is determined by the successful assembly of PEP complex which is composed of plastid-encoded core proteins and its associated proteins (PEP-associated proteins, PAPs) encoded in the nucleus. It has recently been reported that the extensive interactions between proteins composing a PEP complex, such as PEP-PAP or PAP-PAP, are pivotal to establish a functional PEP complex. In this study, an *Arabidopsis* mutant showing whitening and seedling-lethal phenotype was isolated. Genetic and molecular characterization showed that the mutant contains a lesion in *pTAC10/PAP3* gene that encodes an S1 RNA binding domain-containing protein. Expression analyses of *ptac10-1* mutants and *pTAC10*-overexpressing transgenic plants showed that *pTAC10* expression promotes chloroplast development. Interaction analyses between pTAC10 and PEP complex subunits displayed that pTAC10 interacts with PAP proteins including FSD2, FSD3, pTAC7, pTAC14, TrxZ and pTAC10 itself but not with PEP core proteins like rpoA or rpoB. Moreover, interaction analyses using variously truncated pTAC10s showed that the S1 domain is not involved in the pTAC10-PAP interactions although it is essential for pTAC10 function. Rather, C-

terminal region downstream of the S1 domain is responsible for the pTAC10-PAP interactions. Furthermore, introducing DNA constructs overexpressing a series of C-terminal truncated *pTAC10s* could not recover the *ptac10-1* phenotype and induced an abnormal whitening phenotype in the wild type, suggesting that chloroplast development would be disrupted by interrupting the assembly of PEP complex. These observations suggested that pTAC10 plays a decisive role in establishing the functional PEP complex by interacting with other PAPs, which is required for chloroplast development.

Key words **:** chloroplast, chloroplast development, PEP-Associated protein (PAP), Plastid-encoded RNA polymerase (PEP), pTAC10/PAP3

Student Number **:** 2015-23143

Table of Contents

List of Figures

List of Table

Introduction

All photosynthetically active plants have a specialized organelle called chloroplast. Chloroplasts are factories where photosynthesis takes place and indispensable compounds such as fatty acids, amino acids and phytohormones are biosynthesized (Newcomb, 1986; Ravanel et al., 1998; Rawsthorne, 2002; Peltier et al., 2006; Serrano et al., 2016). Genetic and biochemical evidence suggests that the origin of chloroplasts is oxygen-producing photosynthetic bacteria that were engulfed and retained by primitive eukaryotic cells. As reduced to a functional organelle, chloroplast extensively transferred its genome to host nucleus during evolution. These set of events allow chloroplasts to possess own genome and regulatory systems which otherwise is not independent of their nuclear genome (Sagan, 1967; Martin et al., 2002; Pfalz and Pfannschmidt, 2013). In chloroplast genome, there are approximately 100 to 250 genes encoding proteins related to photosynthesis or transcription machinery (reviewed in Wicke et al., 2011). Rather, a majority of proteins in mature chloroplasts are encoded in the nuclear genome and posttranslationally imported from the cytosol. These proteins play diverse roles in chloroplasts, such as regulating gene expression (Abdallah et al., 2000; Soll and Schleiff, 2004).

Plastid genes are mainly transcribed by two distinct types of RNA polymerase, nucleus-encoded RNA polymerase (NEP) and plastid-encoded RNA polymerase (PEP; Hajdukiewicz et al., 1997; Yagi and Shiina, 2014; Yu et al., 2014; Börner et al., 2015). NEP, a single subunit RNA polymerase encoded in the nuclear genome, is mainly responsible for the accurate transcription of plastid housekeeping genes including PEP core subunits (Kapoor et al., 1997; Sakai et al., 1998; Emanuel et al., 2004). In contrast, PEP is the predominating RNA polymerase in chloroplasts which is responsible for massive transcription of photosynthetic genes, most tRNA genes, and rRNA synthesis, according to particular needs (Lgloi and Kössel, 1992; Puthiyaveetil et al., 2010; Zhelyazkova et al.,

2012). This bacterial type, multisubunit RNA polymerase complex is composed of plastid-encoded core subunits called rpoA, rpoB, rpoC1 and rpoC2, and additional proteins such as sigma factors and nuclear-encoded subunits called PEP-associated proteins (PAPs) in *Arabidopsis thaliana*. Genetic analyses using *rpo* knockout mutants demonstrated that these plants have defects in photosynthetic gene expression and chloroplast development (Allison et al., 1996; Santis-Maciossek et al., 1999; Krause et al., 2000).

Protein subunits of the PEP complex have been identified from preparation of both soluble and insoluble fraction in plastids (Bottomley et al., 1971; Hallick et al., 1976; Briat et al., 1979; Pfannschmidt and Link, 1994; Krause and Krupinska, 2000; Majeran et al., 2011; Krupinska et al., 2013; Pfalz and Pfannschmidt, 2013). Recent improvements in proteomic analyses, genomic approaches and protein identification techniques enabled the characterization and identification of plastid proteins more precisely. Since the first preparation of insoluble, membrane-bound fraction designated as plastid transcriptionally active chromosome (pTAC), protein compositions of the plastid RNA polymerase have been identified in *Arabidopsis*, mustard and spinach chloroplasts (Hallick et al., 1976; Reiss and Link, 1985; Little and Hallick, 1988; Krause and Krupinska, 2000; Pfalz et al., 2006; Melonek et al., 2012). Likewise, the proteomic approaches of the soluble fraction like soluble RNA polymerase and nucleoids have reported that additional proteins besides rpos participate in the assembly of PEP complex in mature chloroplasts (Bradley and Gatenby, 1985; Lerbs et al., 1985; Rajasekhar et al., 1991; Pfannschmidt and Link, 1994; Pfannschmidt and Link, 1997). Collectively, these results proposed that the at least 12 PAPs gather together with rpo core subunits to establish a larger PEP complex in mature chloroplasts (Bülow et al., 1987; Loschelder et al., 2004; Pfalz et al., 2006; Steiner et al., 2011; Pfannschmidt et al., 2015).

Previous studies have shown that PAPs are essential in regulating PEP activity and chloroplast development. For instance, genetic analyses using *pap* knockout mutants showed that inactivation of *PAP*s causes albino or pale-green leaves, defects in chloroplast

development, and reduced photosynthetic gene expression. Functional analyses on PAPs also suggested that PAPs play various roles in chloroplasts, such as iron superoxide dismutases, thioredoxin, DNA/RNA-binding proteins, or other reported cellular functions. (Pfalz et al., 2006; Garcia et al., 2008; Myouga et al., 2008; Arsova et al., 2010; Chen et al., 2010; Schröter et al., 2010; Gao et al., 2011; Steiner et al., 2011; Yagi et al., 2012; Huang et al., 2013; Pfalz and Pfannschmidt, 2013; Williams-Carrier et al., 2014; Yu et al., 2014). Kindgren and Strand categorized PAPs according to their functions (Kindgren and Strand, 2015). PAPs in the first group, including pTAC2/PAP2, pTAC3/PAP1, pTAC7/PAP12, pTAC10/PAP3, pTAC12/PAP5, and pTAC14/PAP7, are involved in DNA/RNA metabolism. For example, pTAC3 contains a DNA-binding SAP domain and affects regulation of plastid transcription with PEP complex (Yagi et al., 2012). Precise functions of proteins like pTAC7/PAP12, pTAC12/PAP5 and pTAC10/PAP3 have not been unraveled yet, but several studies have suggested that they are involved in PEP-mediated plastid gene expression and chloroplast development (Pfalz et al., 2006; Kindgren and Strand, 2015). The PAPs in the second group, including pTAC7/PAP12, FLN1/PAP6, FLN2, and TrxZ/PAP10, are regulatory proteins that help transcription by fine-tuning redox status and supporting structural integrity of PEP complex. For instance, FLN1 and its paralogue FLN2 are pfkB-type carbohydrate kinase family members and participate in fine-tuning of PEP transcriptional activity by interacting with other transcription regulatory proteins like TrxZ, a thioredoxin family protein, during chloroplast biogenesis (Arsova et al., 2010; Wimmelbacher and Börnke, 2014). The third group of PAPs, including FSD2/PAP9 and FSD3/PAP4, are involved in the protection of the PEP complex against reactive oxygen species. The superoxide dismutases FSD2 and FSD3 function as a reactive oxygen scavenger to protect PEP complex against oxidative stress (Myouga et al., 2008). The functions of two proteins, pTAC6/PAP8 and MurE-like/PAP11, remain unknown.

Previous biochemical assays have reported that there are extensive interactions between PAP subunits in PEP complex. For example, FLN1 physically interacts with FLN2 and TrxZ together (Arsova et al., 2010; Huang et al., 2013). FSD3 interacts with FSD2 or FSD3 itself to act as a heterodimer or homodimer (Myouga et al., 2008). pTAC7 interacts with FLN1, pTAC10, pTAC12, or pTAC14 (Yu et al., 2013). The interaction between PAP and PEP core subunit was also reported through immunoprecipitation analysis, suggesting that pTAC3 and pTAC14 are associated with an rpo core subunit (Yagi et al., 2012). However, the direct interaction between them has not been verified. A recent model suggested that PEP complex assembly through PAP-PAP or PAP-PEP interactions may be a developmental limiting factor that controls the integrity and activity of the PEP complex as well as chloroplast development (Pfalz and Pfannschmidt, 2013).

Although rapid progress has been made in the understanding of PEP complex in recent years, structure and function of each PAP still remain largely obscure. Thus, it is important to unravel functions of subunit proteins in the PEP complex, as it will contribute to better understanding of chloroplast development and photosynthesis system. pTAC10, an S1 RNA-binding domain protein, has been identified to be an essential PAP responsible for the regulation of PEP activity and chloroplast development (Jeon et al., 2012; Williams-Carrier et al., 2014). Pfalz et al. also reported that pTAC10 is involved in the assembly of the complete PEP complex as a pivotal subunit in maize (Pfalz et al., 2015). Although previous studies reported that pTAC7 interacts with pTAC10 (Steiner et al., 2011; Yu et al., 2013), the interaction between pTAC10 and other PAPs or PEP core subunits in PEP complex is still largely unknown.

Here, a *ptac10* mutant of *Arabidopsis thaliana* displaying a whitening and seedling-lethal phenotype was identified. Phenotypic analyses of the *ptac10* mutant plants and *pTAC10*-overexpressing transgenic plants revealed that pTAC10 plays a pivotal role in PEP-dependent gene expression and chloroplast development. The interaction assay between pTAC10 and other PEP subunits suggested that pTAC10 interacts with at least 6

PAPs including pTAC10 itself. Analysis searching for the domain responsible for the pTAC10-PAP interaction revealed that C-terminal region downstream of the S1 RNA-binding domain is responsible for the interactions, though a previous research suggested that S1 RNA-binding domain is indispensable for transcription stimulating activities of pTAC10 (Jeon et al., 2012). Together with these findings, pTAC10 is a key building block of complete PEP complex and influence PEP-dependent gene expression and chloroplast development.

Material and Methods

Plant materials and growth conditions

In this study, *Arabidopsis thaliana* ecotype Columbia (Col-0) was used as an experimental control. Seeds were surface-sterilized and plated on half-strength MS solid medium. The plates sealed with gas-permeable Micropore® tape were placed at 4℃ in darkness for 2 days and then were moved to a growth chamber under 16-hour photoperiod at 22°C (3M, Minnesota). Seedlings were transplanted from medium to soil for tests on mature plants. *Nicotiana benthamiana* was used as host plants for an agroinfiltration assay. *Nicotiana benthamiana* seeds were sown and grown in soil at a growth chamber under 16-hour photoperiod at 28℃ for 5-6 weeks.

Generation of DNA constructs

Complementary DNA (cDNA) sequences of PAPs were amplified by reverse transcription polymerase chain reaction (RT-PCR) using total RNA extracted from 6-week-old Col-0 leaves. The cDNA of PEP core proteins such as rpoA and rpoB were amplified from chloroplast DNA extracted from chloroplasts of 6-week-old Col-0 leaves. The full-length *pTAC10* cDNA was used to generate the truncated *pTAC10* sequences. For *pTAC10ΔS1*, Gibson Assembly system (New England Biolabs, UK) was used to recombine S1 domain-upstream region and -downstream region. The amplified DNA fragments of *PAPs* and a series of *pTAC10s* were cloned into pDONR221 vector by the BP reaction (Invitrogen, California) to generate entry vectors. The entry vectors were recombined through LR reaction (Invitrogen, California) into adequate destination plasmids to transform plants, analyze protein-protein interaction, or express proteins transiently *in planta*. All the constructs were verified by DNA sequencing.

Generation of transgenic plants and genetic analysis

To generate transgenic plants, the entry clones were recombined into pMDC32 plasmid (Tair Accession Vector: 1009003741), a destination vector containing *CaMV 35s* promoter upstream of the Gateway cassette. The plant binary plasmids were transformed into *Agrobacterium tumefaciens* strain C58C1 by the freeze-thaw method (Holsters et al., 1978). Transformation of Col-0 plants was performed by the *Agrobacterium*-mediated floral dip method (Clough and Bent, 1998). Progenies of the transformed plants were surface sterilized by 70% (v/v) ethanol 5 times and spread onto solid half-strength MS medium containing 0.3% phytoagar (Duchefa, The Netherlands), 50 μg/ml Hygromycin B (Duchefa, The Netherlands), and 100 μg/ml carbenicillin (Duchefa, The Netherlands). Seeds were incubated for 2 days at 4°C in the dark and then placed in a growth chamber with 22°C, 16-hour photoperiod condition. Thirteen to sixteen selected seedlings for each construct were transferred to soil when the second true leaves appeared.

For complementation test, the DNA constructs overexpressing the intact or modified *pTAC10s* were introduced into *ptac10-1* heterogeneous mutants. Progenies of the transformed plants were PCR-genotyped to identify transgenic plants homozygous for the *ptac10-1* allele (for primer sequence, see Supplementary Table 3).

Ultramicrosectioning and transmission electron microscopy

For visualization of chloroplast ultrastructure, ultramicrosectioning was conducted as described previously by Motohashi et al. (2001) with slight modifications (Motohashi et al., 2001). Leaves of 1-, 3-, 6-, and 10-week-old plants were collected. Samples were fixed with fixation solution I [0.86 M Na-P (pH 7.2), 1% paraformaldehyde (w/w), and 1% glutaraldehyde (w/w)] for 24 hours at room temperature and then washed 3 times with washing solution [0.137 M Na-P (pH 7.2)]. Samples were post-treated in fixation solution II [0.86 M Na-P (pH 7.2) and 2% osmium tetroxide (w/w)] for 1 hour at room temperature,

washed 3 times, dehydrated in a graded acetone series [25%, 50%, 75%, and 100% in distilled, deionized water (v/v)], and sequentially infiltrated in a series of Spurr's epoxy resin (Sigma) [25%, 50%, 75%, and 100% in acetone (v/v)]. For solidification, embedded samples were placed at 65℃ for 2 days. Ultrasections were obtained using an ultramicrotome (EM UC7; Leica, Germany). Images were observed and generated by a transmission electron microscope (TEM) (JEM1010; JEOL, Massachusetts).

Yeast two-hybrid assay

To perform the yeast two-hybrid assay (Y2H), Matchmaker Gold Yeast Two-Hybrid System (Clontech, California) was used to generate Y2H constructs. pGBKT7 vector carries a bait protein-fused GAL4 DNA-binding domain and pGADT7 vector contains a prey protein-fused GAL4 activation domain. The cDNA of the full-length or truncated *pTAC10*s and PEP subunits were fused in-frame with GAL4 DNA-binding or activation domain using *Sma*I restriction site within pGBKT7 and pGADT7 through Gibson Assembly System (New England Biolabs, UK), respectively. The bait plasmids containing the intact or modified *pTAC10*s and prey plasmids encoding *PAP*s were cotransformed into Y2H Gold yeast (*Saccharomyces cerevisiae*) strain to analyze protein-protein interactions. Cotransformed yeast lines were plated on double dropout minimal medium lacking leucine and tryptophan (DDO, -Leu/-Trp) and incubated for 2 days at 30℃ in the dark. The selected yeast lines were diluted to an OD_{600} of 0.05 and inoculated on DDO medium containing aureobasidin A (Abs A, 250 ng/ml) or quadruple dropout medium lacking leucine, tryptophan, adenine and histidine (QDO, -Leu/-Trp/-Ade/-His). The yeast lines were also inoculated on DDO medium to verify yeast transformation and equal dropping. The plates were incubated for 2 days at 30℃ in darkness. Images of the plates were taken by a digital camera (Coolpix p300; Nikon, Japan). (for primer sequence, see Supplementary Table 3).

In vitro pull-down assay

To generate GST-fused *pTAC10* and MBP-fused *PAP* expression clones, entry clones containing pTAC10 and PEP subunits were recombined into pGEX-DC and pMAL-DC destination vectors, respectively (Zhang et al., 2005). All expression clones were introduced into the *Escherichia coli* BL21 (DE3) pLysS strain, and protein expression was induced by 0.5 mM isopropyl-b-D-thiogalactoside at 18°C overnight. After induction, cells were harvested and sonicated in homogenization buffer [25 mM Tris-HCl (pH 7.5), 0.5% Triton X-100, 150 mM NaCl, and 2 mM EDTA]. GST and GST-pTAC10 proteins were incubated for 4 hours at 4°C with glutathione-Sepharose 4B beads (GE Healthcare, Chicago) with gentle rotation. Beads were washed 3 times with washing buffer [25 mM Tris-HCl (pH 7.5), 150 mM NaCl, and 2 mM EDTA] and incubated together with MBP-fused PAP proteins. Beads were washed 3 times again and eluted by boiling with 2×sample buffer. For immunoblot, the protein samples were loaded onto 10% SDS-PAGE gel and transferred to a polyvinylidene fluoride membrane (Bio-Rad, California). After overnight incubation with MBP polyclonal antibodies (Santa Cruz, Texas), anti-rabbit HRP-linked secondary antibody (Thermo Fisher, Massachusetts) was applied for 3 hours at room temperature. The proteins were visualized by chemiluminescence lighting using an Amersham ECL prime (GE Healthcare, Chicago) and monitored using a LAS-3000 imaging system (Fujifilm, Japan).

Tissue culture and transformation of calli

Tissue culture and transformation of calli were performed as described by Akama et al. (1992) with slight modifications (Akama et al., 1992). Col-0 plants and *ptac10-1* mutants were grown for 10 days under sterile conditions as described above. Roots were cut at 5 to 10 mm from the root tip and incubated on CIM medium [Gamborg's B5 medium, 20 g/L glucose, 0.5 g/L MES, 0.1 mg/L kinetin, 0.5 mg/L 2,4-D, and 0.5% agar] for 6 days.

Incubated calli were soaked in a suspension of the *Agrobacterium tumefaciens* strain C58C1 (OD600 = 0.2) containing constructs for transformation in AIM [Gamborg's B5 medium, 0.5 g/L MES, 0.894 mg/L 2-isopentenyladenine, and 0.093 mg/L NAA]. Most of the liquid was removed and then calli were cultured for 2 days at 23℃ under continuous light. Calli were washed 10 times with AIM containing 300 mg/L kanamycin. The washed calli were incubated on SIM medium [Gamborg's B5 medium, 20 g/L glucose, 0.5 g/L MES, 0.894 mg/L 2-isopentenyladenine, 0.093 mg/L NAA, and 0.5% agar] containing 20 mg/L Hygromycin B at 23℃ under continuous light. The incubated calli were transferred to new SIM medium every 2 weeks.

Agroinfiltration of *Nicotiana benthamiana* leaves

To test protein-protein interaction *in planta*, *pTAC10*, cDNAs of *pTAC10ΔS1* and *FSD3* were inserted into pE2C and pE3C entry vectors using Gibson Assembly system to generate C-terminal HA- or myc-tagged fusion protein (Dubin et al., 2008). The *pTAC10-HA*, *pTAC10ΔC-HA* and *FSD3-myc* recombinant DNA were inserted into pMDC32 destination vector to generate 35s::pTAC10-HA, 35s::pTAC10ΔC-HA and 35s::FSD3-myc expression clones.

Agrobacterium injection was performed as described previously by Llave et al. (2000) with slight modifications (Llave et al., 2000). *Agrobacterium tumefaciens* strain C58C1 was transformed with 35s::pTAC10-HA, 35s::pTAC10ΔC-HA and 35s::FSD3-myc by freeze-thaw method, respectively (Holsters et al., 1978). Individual *Agrobacterium* colonies were grown for 24 hours at 28℃ in 5 ml culture medium [Luria broth, 100 μg/ml rifampicin and 50 μg/ml kanamycin]. This was used to inoculate 250 ml of culture medium [Luria broth, 20 μM acetosyringone, 10 mM MES (pH 5.7) with 100 μg/ml rifampicin] at 28℃ for 24 hours. The cells were collected by centrifugation, resuspended in infiltration buffer [10 mM $MgCl_2$, 10 mM MES (pH 5.7), and 200 μM acetosyringone] to OD_{600} of 0.5, and incubated at 28℃ for 3 hours. By using 1 ml syringe, resuspended cells were

injected into leaves through small holes created by a yellow tip. Infiltrated leaves were collected 3 days after injection.

Co-immunoprecipitation assay

For co-immunoprecipitation (Co-IP) analysis, collected *Agrobacterium*-infiltrated leaves were ground in liquid nitrogen and resuspended in immunoprecipitation buffer [50 mM Tris-HCl (pH 7.5), 150 mM NaCl, 10 mM $MgCl_2$, 0.1% Nonidet P-40 (v/v), 1 mM phenylmethylsulfonyl fluoride, 10% glycerol (v/v), 1 mM DTT, and protease inhibitor cocktail (Roche, Switzerland)] to extract total proteins. After centrifugation at 13,000 rpm for 15 min, the supernatant was incubated with HA polyclonal antibodies (Thermo Fisher, Massachusetts) at 4℃ for 2 hours. Protein A agarose (Thermo Fisher, Massachusetts) was used to pull-down immune complexes. The mixture was incubated at 4℃ overnight and then washed 4 times with immunoprecipitation buffer lacking Nonidet P-40. For immunoblot, processes were performed as described above, except myc monoclonal antibodies (Thermo Fisher, Massachusetts) as a primary antibody and anti-mouse HRP-linked secondary antibodies (Thermo Fisher, Massachusetts).

Gene expression Analysis

Total RNA of Col-0, *ptac10-1* mutants and *pTAC10*-overexpressing plants were extracted by RNeasy plant mini-prep kit (Qiagen, Germany) according to the manufacturer's instruction. The 20 μg of the extracted RNA was reverse transcribed using Superscript III to synthesize the first-strand cDNA and then diluted 10-fold. For quantitative reverse transcription-PCR (qRT-PCR), cDNA template, primers for qRT-PCR, the LightCycler 480 SYBR GREEN I Master Mix (Roche, Switzerland) and water were mixed according to the manufacturer's instructions, and the qRT-PCR was performed as follows: initial denaturation at 95°C for 5 min followed by 45 cycles of denaturation at 95°C for 10 sec,

annealing at 58°C for 10 sec, and extension at 72°C for 10 sec. The signals were detected by a Light Cycler NANO Real-Time PCR machine (Roche, Switzerland). All qRT-PCR assays were run with an internal control AtACT2 (At3g18780) and performed in technical replicates of three to analyze expression levels (for primer sequence, see Supplementary Table 3).

Leaf Chlorophyll Measurement

To measure chlorophyll contents in 6-week-old Col-0 and *pTAC10*-overexpressing plants, chlorophyll concentration measurement was performed as previously described by Sumanta et al. (Sumanta et al., 2014). Twenty-fold of 95% ethanol in distilled, deionized water (w/v) was added to homogenized fresh leaves and incubated 24 hours at 4℃. The samples were centrifuged at 12000 rpm for 15 min at 4℃. The supernatants were diluted 10-fold 95% ethanol. A UV/visible spectrophotometer (OPTIZEN POP; Mecasys) was used to measure absorbance at 664 nm, 649 nm, and 470 nm to calculate chlorophyll a, chlorophyll b and total chlorophyll concentrations. An SPDA-502 chlorophyll meter (Konica Minolta, Japan) was used to measure chlorophyll contents directly.

RNA Sequencing Analysis

Total RNA was extracted from shoot part of 7-day-old Col-0 and *ptac10-1* mutant seedlings grown on half-strength MS media at normal growth condition using the RNeasy plant mini-prep kit (Qiagen, Germany) with DNase I treatment to remove DNA contaminant. The RNA samples were subjected to quantity and quality assessment by Agilent Technologies 2100 Bioanalyzer (Agilent Technologies, California). The Truseq RNA library kit was used to construct cDNA libraries, according to the manufacturer's instruction. Briefly, mRNA from total RNA was isolated, purified, fragmented, cDNA-synthesized and ligated with adapters. The generated double-stranded cDNA was purified

for end repair, dA tailing, adapter ligation, and enrichment. Then the libraries were sequenced using the Illumina HiSeq2000 platform (Illumina, California). Enrichment of the transcript sequencing data was calculated as fragments per kilobase of exon model per million mapped reads of each transcript in each sample by Cufflinks software. The transcripts whose expression is zero in at least one sample were removed from each dataset. The multi-experiment viewer MeV, part of the TM4 microarray software suite, was used for the generation of heat maps (Saeed et al., 2006). The accession number of these datasets is GSE90159 (https://www.ncbi.nlm.nih.gov/geo/query/acc.cgi?acc= GSE90159).

Accession Numbers

Sequence data from this article can be found in the Arabidopsis Genome Initiative or GenBank/EMBL databases under the following accession numbers: pTAC10 (At3G48500), pTAC2 (At1G74850), pTAC6 (At1G21600), pTAC7 (At5G24314), pTAC12 (At2G34640), pTAC14 (At4G20130), FSD2 (At5G51100), FSD3 (At5G23310), TrxZ (At3G06730), MurE-like (At1G63680), rpoA (AtCG00740), rpoB (AtCG00190), rbcL (AtCG00490), psbA (AtCG00020), psaB (AtCG00340), and psbD (AtCG00270).

Results

Identification of *ptac10-1* mutant with seedling-lethal and whitening phenotype

A T-DNA insertion mutant exhibiting defects in leaf greening and growth was isolated (Fig. 1, A, D and E). Phenotypic analysis of the mutant showed that the color of cotyledons turned white by 3 days after germination and the growth arrest occurred in a seedling stage, approximately 7 days after germination even though they were supplemented with sucrose as a carbon source (Fig 1, A-C). Morphological analysis of the seedlings and protoplasts showed that the mutants have plastids that do not differentiate into chloroplasts (Fig 1, D-G). In more detail, protoplasts isolated from the wild-type plants appeared to have thylakoid membranes distributed throughout chloroplasts. In contrast, protoplasts isolated from mutant cotyledons showed no green area and abnormal plastids which were not observed in wild-type plants, indicating chloroplast development was severely disrupted in this mutant.

To examine the developmental status of the chloroplast in the mutant, chloroplasts in cotyledons of wild-type and the mutant plants were analyzed by TEM (Fig. 1, H-M; Fig. S1). Chloroplasts in the wild type contained well-organized thylakoid membranes with many grana stacks, whereas the whitened cotyledons of the mutants contained abnormal plastids lacking stacks of thylakoid membranes. This suggested that chloroplast development in this mutant is severely compromised. Altogether, these observations indicated that the mutant may have a defect in one of the genes responsible for chloroplast development.

To identify the candidate gene responsible for this phenotype, the flanking sequences of the genomic location where T-DNA insertion occurred were analyzed through flanking sequence tag method (Thole et al., 2009). Sequencing results of the obtained flanking

sequences indicated that *pTAC10* was a candidate gene causing the mutation. To further confirm whether the phenotype was induced by suppressed expression of *pTAC10*, PCR-based genotyping, genetic analysis, expression analysis, and genomic complementation analysis on the mutants were performed (Fig. 2). The genotype results showed that the mutants with whitened cotyledons were homozygous for the T-DNA insertion (Fig. 2, A and B). Since the homozygous mutants were seedling-lethal, the mutant was maintained as a heterozygous line. Progeny of a self-pollinated heterozygous mutant segregated green and albino plants in approximately 3:1 ratio (green:white seedlings = 185:56) on a non-selective medium. The segregation ratio of homozygous wild-type and heterozygous mutant was also close to 1:2 in randomly selected seedlings with green leaves (homozygous wild-type:heterozygous mutant seedlings = 5:11), suggesting that the genotype is linked to the mutant phenotype (Fig. 2, C). Expression level of *pTAC10* in the homozygous mutants was approximately 5-fold lower than that in the wild type (Fig. 2, D). In the homozygous mutants, expression levels of PEP-dependent photosynthetic genes, such as *psaA*, *psbA*, *psaB*, and *rbcL* were significantly decreased, whereas NEP-dependent genes like *rpoA* and *rpoB* were increased significantly (Fig. S2; Table S1). These results implied that this mutant phenotype was derived from the suppressed expression of *pTAC10*.

To check whether introducing the intact *pTAC10* can rescue the mutant phenotype, the full-length cDNA of *pTAC10* was introduced into the mutant plants (Fig. 2, E). The mutant phenotype was rescued by the introduction of the full-length *pTAC10*. These results demonstrate that the mutant phenotype is caused by disruption of *pTAC10* expression, indicating pTAC10 plays an essential role in the complete PEP activity and chloroplast development. This new mutant allele was named *ptac10-1*.

The *pTAC10* expression is involved in chloroplast development and leaf greening

The phenotype of homozygous *ptac10-1* mutants showed that pTAC10 is indispensable for chloroplast development, and that of heterozygous *ptac10-1* mutants also displayed the importance of pTAC10 in chloroplast development as well. The heterozygous *ptac10-1* mutants showed pale-green leaves and relatively inhibited growth compared to those of homozygous wild-type plants (Fig. 3, A; Fig. S3, A and B). When the structure of chloroplasts was observed by TEM, chloroplasts in the *ptac10-1* heterozygous mutants contained more stacks of thylakoid membranes than the homozygous mutants had. However, the thylakoid membranes in chloroplasts of the heterozygous mutants were severely disorganized compared to those of the wild type (Fig. 3, B).

The expression level of *pTAC10* in heterozygous mutants was approximately half of the wild-type plants (Fig. 3, C; Fig. S3, C). Together with the results of homozygous *ptac10-1* mutant and wild-type plants, these data suggested that pTAC10 is pivotal for chloroplast development as well as its expression level appears to be roughly proportional to the degree of leaf coloration and chloroplast development.

pTAC10 expression is regulated in a light-responsive manner

To identify the relationship between *pTAC10* expression and leaf developmental stages, the expression levels of *pTAC10* transcripts in wild-type leaves were analyzed at four developmental time points: 1, 3, 6, and 10 weeks after germination (Fig. 4, A and B). The results showed that *pTAC10* expression was altered according to leaf developmental stages. The *pTAC10* expression level was approximately 6-fold higher in 3-week-old rosette leaves than in 1-week-old cotyledons. The *pTAC10* expression was highest in 6-week-old mature leaves but significantly suppressed in 10-week-old senescing leaves. This data indicated that the *pTAC10* expression is correlated to the developmental stages of chloroplasts and leaves.

Gene expression analyses using qRT-PCR with RNA extracted from aerial and underground parts of wild-type plants demonstrated that *pTAC10* expression is higher in

shoot than root (Fig. 4, C). This suggested that pTAC10 is mainly expressed in leaves and there is a correlation between *pTAC10* expression and chloroplast development. To further analyze the effect of the *pTAC10* expression in response to light, qRT-PCR analysis was performed to measure transcript levels of *pTAC10* in light and dark conditions. The wild-type plants grown in the light condition showed approximately 2.5-fold higher expression level of *pTAC10* than plants grown in the dark condition (Fig. 4, D). These results indicated that *pTAC10* expression has correlation with chloroplast development and leaf greening in both developmental stage-dependent and light-dependent manner.

Overexpression of *pTAC10* affects chloroplast and plant development

To investigate the function and effect of pTAC10 in chloroplast development and leaf greening, *pTAC10*-overexpressing DNA construct was introduced into Col-0. Overexpression of *pTAC10* in wild-type plants influenced plant growth on several aspects. The transgenic plants overexpressing *pTAC10* had deeper green leaves than those of wild-type plants, although both transgenic and wild-type plants grew under the same conditions (Fig. 5, A). Quantification of chlorophyll concentration demonstrated that overexpression of *pTAC10* causes the transgenic plants to contain higher chlorophyll contents than wild-type plants. When comparing 6-week-old plants, *pTAC10*-overexpressing plants displayed an approximately 35% increase in chlorophyll contents compared to the wild type (Fig. 5, B). Similarly, 2-week-old *pTAC10*-overexpressing plants contained 17% to 22% higher chlorophyll contents than Col-0 plants (Fig. 5, C).

Overexpression of *pTAC10* also affected the de-etiolation process. Etiolated seedlings of wild-type and *pTAC10*-overexpressing plants grown in the dark were exposed to continuous light, and chlorophyll contents were calculated in a time-course manner to compare the greening rate (Fig. 5, D). We found that the chlorophyll contents of *pTAC10*-

overexpressing plants were significantly higher than those of the wild-type after 12 hours of light exposure (Fig. 5, E and F). These data demonstrated that greening of leaves in *pTAC10*-overexpressing transgenic plants is faster than that of wild-type plants.

To ascertain whether overexpression of *pTAC10* affects chloroplast development, protoplasts were isolated from *35s::pTAC10* and wild-type plants, respectively (Fig. 6, A-C). Comparison between the transgenic and wild-type plants showed the number of chloroplasts per protoplast was significantly different in wild-type and *35s::pTAC10* plants. Some protoplasts isolated from *pTAC10*-overexpressing plants were fully filled with numerous chloroplasts, which was not observed in Col-0 plants (Fig. 6, A). The average number of chloroplasts per protoplast was around 28 in Col-0, whereas it was around 50 in protoplast isolated from *pTAC10*-overexpressing transgenic plants ($n > 80$ protoplasts; Fig. 6, B). Frequency distribution displaying the number of chloroplasts per protoplast also depicted the differences graphically (Fig. 6, C). In Col-0, the most of the data was centered between 20 and 30 and 92% of protoplasts contained less than 40 chloroplasts. However, the distributions of the *35s::pTAC10* transgenic plants showed shifts to the right compared to the wild-type. In the transgenic plants, around 50% of protoplasts contained more than 40 chloroplasts. Despite the differences in chloroplast number, ultrastructures of chloroplasts in *35s::pTAC10* and wild-type plants were hardly distinguishable (Fig. 6, D).

When the expression of chloroplast genes was analyzed in the two independent lines of *pTAC10*-overexpressing transgenic plants and Col-0 plants, PEP-dependent genes such as *psaA*, *psbA*, *psaB*, and *rbcL* were increased significantly while NEP-dependent genes like *rpoB* did not show a remarkable difference (Fig. 6, E). To further examine the relation between *pTAC10* expression and PEP-dependent gene expression, we analyzed expression of *rbcL* in four independent lines of *pTAC10*-overexpression transgenic plants (Fig. S4, C and D). The results displayed that expression level of *rbcL* was higher than that of wild-type plants in all the *pTAC10*-overexpressing plants. Moreover, *pTAC10* expression level

showed a positive correlation with *rbcL* expression level. Nonetheless, since there was still a possibility that this effects might not be specifically caused by *pTAC10* overexpression, *rbcL* expression was analyzed in plants overexpressing another PAP gene, *FSD3*. Unlike *35s::pTAC10* plants, the phenotype and chlorophyll contents of *35s::FSD3* transgenic plants were hardly distinguishable compared to those of wild-type plants (Fig. S4, A and B). Furthermore, transgenic plants with various *FSD3* expression levels did not show a noticeable correlation between *FSD3* expression level and *rbcL* expression level (Fig. S4, C and D). These suggested that pTAC10 is a limiting factor that regulates PEP activity among PAPs.

As per the observations, overexpression of *pTAC10* triggered improvement of biomass and productivity and abnormal developmental responses including leaf development. The transgenic plants displayed a 1.1- to 1.25-fold increase in total dry weight and seed weight while their apical growth was not significantly altered compared to the wild-type plants grown in the same conditions (Table 1). Overexpression of *pTAC10* also led to leaf development abnormalities that did not occur in wild-type plants (Fig. 7, A and B). Two to seven percent of leaves collected from *pTAC10*-overexpressing plants displayed various abnormal leaf structures, such as a forked snake tongue-like shape or a severely wrinkled shape that was not observed in the wild-type grown in the same conditions. These findings suggested that the overexpression of *pTAC10* affects chloroplast development, which might affect leaf morphology and development. This was supported by previous studies that chloroplast development is involved in leaf morphology (Moschopoulos et al., 2012; Mateo-Bonmatí et al., 2015). To better understand the molecular basis underlying this abnormal morphology, transcript levels of the genes like *AS1*, *AS2*, *KAN1*, *ARF3*, and *YAB5* was analyzed, which are known to be involved in leaf morphology regulation (Fig. 7, D). Previous studies reported that *AS1* and *AS2* promote adaxial identity while *KAN1*, *ARF5* and *YAB5* contribute to the specification of abaxial cell fate (Machida et al., 2015; Matsumura et al., 2016). Mutation in these genes caused abnormal leaf structures such as

dome-, trumpet-, needle-, or leaflet-shaped leaves (Siegfried et al., 1999; Kerstetter et al., 2001; Lin et al., 2003; Eshed et al., 2004; Pekker et al., 2005; Iwakawa et al., 2007; Husbands et al., 2015). The results of the expression analyses in the abnormal leaves collected from *pTAC10*-overexpressing plants showed *AS1* and *AS2* expression level was downregulated and *KAN1* expression was upregulated. On the other hand, expression patterns seemed to be opposite in the *ptac10-1* mutants showing upregulation of *AS1* and *AS2* expression and downregulation of *KAN1* expression (Fig. 7, E). These implied that *AS1*, *AS2* and *KAN1* might be involved in the formation of abnormal leaf morphology in *35s::pTAC10* transgenic plants. Moreover, though there was altered gene expression of genes involved in leaf shape in the *35s::pTAC10* plants, morphologies of the leaves collected from *pTAC10*-overexpressing plants were different from previously reported abnormal leaf shapes. This suggested that signaling from chloroplasts might be involved in leaf morphology through a different pathway.

The interaction between pTAC10 and various PAPs

Previous studies reported that *pap* knockout mutants displayed whitening or pale-green phenotypes and severely suppressed PEP activity (Pfalz et al., 2006; Garcia et al., 2008; Myouga et al., 2008; Arsova et al., 2010; Schröter et al., 2010; Gao et al., 2011; Steiner et al., 2011; Yagi et al., 2012; Williams-Carrier et al., 2014). This suggested that the expression of *PAP*s might play a critical role in the regulation of PEP activity and chloroplast development. However, the *ptac10-1* mutants showed upregulated *PAP* expressions, whereas *pTAC10*-overexpressing transgenic plants displayed downregulated *PAP* expressions (Fig. 8, A and B; Table S2). These findings implied that the transcriptional regulation of *PAP*s does not bring about the phenotypes of *ptac10-1* and *35s::pTAC10* plants.

Recent studies suggested that PAPs are indispensable to establish the PEP complex (Pfalz et al., 2015). Although previous studies identified some PAP-PAP interactions like

pTAC10-pTAC7 interaction in PEP complex (Yu et al., 2013), the interaction of pTAC10 with other PEP components has largely remained unknown. To explore the interaction between pTAC10 and other subunits composing PEP complex, we performed Y2H assays using pTAC10 as bait and other PEP complex components as prey (Fig. 8, C-F). Yeast lines cotransformed with the pTAC10 bait plasmid and the prey plasmids encoding FSD2, FSD3, TrxZ, pTAC7, pTAC14 and pTAC10 itself survived in the QDO media (Fig. 8, C). The yeast lines cotransformed with the *pTAC10* bait plasmid and prey plasmids encoding rpoA core subunits, MurE-like, pTAC2, pTAC6, and pTAC12 failed to survive in the same growth conditions. This result was also verified by additional Y2H assay using the DDO containing Abs A (Fig. 8, D), whereas all the cotransformed yeast lines survived on the DDO control medium (Fig. 8, E). To test autoactivation, the empty bait plasmid (Blank) was used to cotransform the yeast lines with the *PAP* prey plasmids, and there was no yeast line survived on Abs A-containing DDO medium (Fig. 8, F). These results showed that pTAC10 interacts with PAPs belonging to the various groups: pTAC7, pTAC14 and pTAC10 itself (group 1), TrxZ (group 2), FSD2 and FSD3 (group 3).

GST pull-down assay was performed to further examine the binding of pTAC10 and PEP subunits (Fig. 8, G). GST-tagged pTAC10 and MBP-tagged PAPs, such as MBP-pTAC7, MBP-TrxZ, and MBP-FSD3, were extracted from *Escherichia coli* strain BL21(DE3) pLysS and purified to homogeneity. These purified proteins were then subjected to pull-down assay using GST-pTAC10 or GST alone as bait and MBP-fused PAPs or MBP alone as prey proteins. The GST-pTAC10 successfully pulled down the MBP-fused pTAC7, TrxZ and FSD3, respectively while the MBP alone was not pulled down. In contrast, the GST alone did not pull down any of bait proteins, confirming our findings that pTAC10 interacts with a broad range of other PAPs.

Kindgren and Strand recently suggested that group 1 PAPs, proteins with DNA- or RNA-binding ability, might play a potential role in linking transcription to translation (Kindgren and Strand, 2015). Since pTAC10 is one of the PAPs belonging to the group 1

PAPs, pTAC10 might interact with proteins associated with the translation process. Therefore, Y2H assay was performed to analyze the interaction between pTAC10 and proteins involved in the plastid translational machinery, such as 30S ribosomal protein S3, 50S ribosomal protein L12-1, 50S ribosomal protein L29, and plastid elongation factor Tu in *Arabidopsis* (Ristic et al., 2007; Fleischmann et al., 2011; Pfalz and Pfannschmidt, 2013). However, all the yeast lines cotransformed with the bait plasmid encoding pTAC10 and the translation component-encoding prey plasmids did not survive in DDO medium including Abs A. This suggested that pTAC10 do not interact with these 4 components of the plastid translational machinery.

C-terminal region of pTAC10 is responsible for pTAC10-PAP interactions.

pTAC10 contains an S1 RNA-binding domain of about 70 amino acids in the middle of the protein (Fig. 9, A). A recent study reported that S1 RNA-binding domain of a tobacco pTAC10 homologue plays an indispensable role in regulating photosynthetic gene expression and chloroplast development (Jeon et al., 2012). Furthermore, overexpression of *pTAC10* without S1 domain (pTAC10ΔS1) could not rescue the homozygous *ptac10-1* phenotype (Fig. S5). This suggested that the S1 domain might be involved in the interaction between pTAC10 and other PAPs to establish a functional PEP complex. To verify the hypothesis, Y2H assay using *PAP* prey plasmids and variously truncated *pTAC10* bait plasmids was performed (Fig. 9). All the yeast lines transformed with the bait plasmids of the truncated *pTAC10* carrying the N-terminal region upstream of the S1 domain (pTAC10N), S1 domain only (pTAC10S1), or both N-terminal region and S1 domain (pTAC10NS1) did not survive on the Abs A-including DDO medium. This indicated that N-terminal region and S1 domain are not a domain mediating the pTAC10-PAP interactions. On the other hand, all the yeast lines transformed with the bait plasmid

containing the C-terminal region downstream of the S1 domain (pTAC10C) showed autoactivation, which suggested that the C-terminal region might mediate the pTAC10-PAP interactions and the deletion of the N-terminal region causes autoactivation.

To characterize the region mediating the interactions more precisely, bait plasmids carrying a series of C-terminal truncated fragments of *pTAC10* containing the intact N-terminal region and S1 domain were generated (Fig. 10, A). Yeast lines transformed with these C-terminal truncated *pTAC10* bait plasmids did not show autoactivation as well as displayed interactions with PAPs (Fig. 10, B). Yeast lines cotransformed with the bait plasmid carrying *pTAC10-1245* and the prey plasmid containing *TrxZ* or *pTAC7* survived in Abs A-containing DDO medium, indicating the C-terminal region containing amino acids 341 to 415 mediates the pTAC10 interaction with TrxZ and pTAC7. As the longer the C-terminal regions of *pTAC10* were, the more pTAC10-PAP interactions were observed. Y2H assay using the pTAC10-1467 bait plasmid amino acids displayed the pTAC10 interaction with TrxZ, pTAC7 or the intact pTAC10. Likewise, pTAC10-1470 showed additional interactions with pTAC14 and FSD3. These data indicated that pTAC10 C-terminal region of amino acids 341 to 415 mediates pTAC10 interaction with pTAC7 and TrxZ, the region containing amino acids 416 to 489 mediates the interaction with pTAC10 itself, the region containing amino acids 490 to 580 can interact with pTAC14 and FSD3, and the region containing amino acids 581 to the end mediates interaction with FSD2. Altogether, these indicated that pTAC10 C-terminal region downstream of the S1 domain is responsible for the pTAC10 interaction with other PAPs. Co-IP analysis of pTAC10 and FSD3 partially supported these interactions (Fig. 10, C). The full-length pTAC10 can bind to FSD3 whereas pTAC10 without the C-terminal region downstream of the S1 domain (pTAC10ΔC) failed to bind with FSD3.

To examine the importance of interactions between pTAC10 and PAPs *in planta*, homozygous *ptac10-1* mutants were transformed with a series of C-terminal truncated *pTAC10*-overexpressing plasmid named 35s::pTAC10-1245, 35s::pTAC10-1467, and

35s::pTAC10-1740. Phenotypic analyses of these transgene-introduced *ptac10-1* mutants showed that the truncated *pTAC10*s could not recover the mutant phenotype (Fig. 10, D). This indicated that the C-terminal region of pTAC10 is critical for the interactions between pTAC10 and PAPs, and also suggested that the complete interactions between pTAC10 and PAPs in PEP complex are essential in chloroplast development.

If the C-terminal truncated pTAC10 existed in the wild type, the interactions between endogenous pTAC10 and PAPs might be able to be interfered due to a dominant negative effect, which could affect complete PEP complex formation and chloroplast development. To test this hypothesis, transgenic plants overexpressing *pTAC10-1245*, *pTAC10-1467*, and *pTAC10-1740* in the Col-0 background were generated. These transgenic plants displayed that abnormal whitening phenotypes that were not observed in the wild type (Fig. 11, A-J). The abnormal whitening phenotype was observed in 3 out of 15 independent transgenic lines of *35s::pTAC10-1467* (25%) and 4 out of 13 independent lines of *35s::pTAC10-1740* (31%). However, the abnormal whitening phenotype was not observed in any of *35s::pTAC10* (8 lines) and *35s::pTAC10-1245* (15 lines) plants. The abnormal whitening phenotype suddenly emerged in several organs like rosette leaves, petioles, cauline leaves, and stems, at various developmental stages.

Structure of plastids in the green and white parts of the leaves with whitening was observed through TEM (Fig. 11, K-O; Fig. S6). In the green area, chloroplasts were almost identical to those of Col-0, showing well-organized stacks of thylakoid membranes. However, the plastids in the whitened part did not show proper stacks of thylakoid membranes. When analyzing the expression levels of the truncated *pTAC10* transgenes and the endogenous *pTAC10*, their expression levels were similar between the transgenic plants with and without the abnormal whitening phenotype (Fig. S7, A and B). Furthermore, in abnormal whitening-occurred leaves, the expression level of endogenous *pTAC10* in the green part was slightly higher than that in whitened part (Fig. S7, C and D). These suggested that this whitening phenotype might not be caused by gene silencing of

endogenous *pTAC10* but might be induced by disrupted functions of endogenous pTAC10. Collectively, these observations suggested that the pTAC10-PAP interaction mediated through the C-terminal region is pivotal for PEP complex formation as well as the assembly of the PEP complex might be involved in plastid signaling.

Discussion

In this study, a mutant allele named *ptac10-1* was identified whose expression of *pTAC10/PAP3* is suppressed. pTAC10 was first identified in *Arabidopsis* as a component of the TAC proteins and considered as a PAP due to its tight association with the PEP core subunits (Pfalz et al., 2006; Steiner et al., 2011). Recent studies suggested that PAPs govern the activity of PEP by establishing the PEP complex and this assembly is a developmental bottleneck regulating chloroplast development (Pfalz and Pfannschmidt, 2013). Many studies on *pap* mutants showed plants with disrupted *PAP* expression displayed albino or pale-green phenotypes, inhibited chloroplast development and reduced expression of PEP-dependent plastid genes, which was also reported in loss-of-function *rpos* mutants (Hess et al., 1993; Allison et al., 1996; Santis-Maciossek et al., 1999; Krause et al., 2000; Legen et al., 2002; Pfalz et al., 2006; Garcia et al., 2008; Myouga et al., 2008; Arsova et al., 2010; Gao et al., 2011; Gilkerson et al., 2012; Yagi et al., 2012; Yu et al., 2013; Pfalz et al., 2015; Yu et al., 2018). This phenomenon was also observed in *ptac10-1* mutants, supporting that PEP activity is regulated by PAPs.

Previous studies showing the interaction of PAP-PAP or PAP-PEP also supported the idea that PAPs play a pivotal role in regulating the activity of PEP complex and chloroplast development (Arsova et al., 2010; Gao et al., 2011; Yagi et al., 2012; Huang et al., 2013; Yu et al., 2013). Though pTAC10 did not bind to PEP core subunits or the isolated 4 translational machinery subunits, pTAC10 showed a wide range of interactions with at least 6 of PAPs including FSD2, FSD3, pTAC7, pTAC14, TrxZ and pTAC10 itself. The identified PAPs interacting with pTAC10 belonged to three different groups according to the functional categorization of the PAPs (Kindgren and Strand, 2015). pTAC7 and pTAC14 belong to the group 1, TrxZ belongs to group 2, and FSD2 and FSD3 belong to the group 3. These suggested that pTAC10 plays an essential role in the establishment of

functional PEP complex, supported by a recent model that pTAC10 may control PEP activity by controlling the establishment of functional PEP complex (Pfalz et al., 2015).

A single S1 binding domain is located in the middle of pTAC10, suggesting pTAC10 has an RNA-binding potential. Recent studies reported that pTAC10 directly binds to plastid RNA in a non-specific manner and the RNA-binding affinity of pTAC10 is promoted by phosphorylation (Jeon et al., 2012; Yu et al., 2018). These studies revealed that the significance of the S1 domain for pTAC10 function in PEP-dependent gene expression. In this study, however, the interaction assays disclosed that the domain responsible for pTAC10-PAP interactions is not the S1 domain or the N-terminal region upstream of the S1 domain but the C-terminal region downstream of the S1 domain. The Y2H assays using the series of C-terminal truncated pTAC10s containing N-terminal and S1 domain showed that C-terminal region downstream of the S1 domain is responsible for the interactions between pTAC10 and PAPs.

Based on the idea that PAP-PEP and PAP-PAP interactions mediate the formation of PEP complex, pTAC10-PAP interactions through the C-terminal region of pTAC10 might be key to the establishment of PEP complex and chloroplast development. To address this, the constructs overexpressing C-terminal truncated *pTAC10*s, such as 35s::pTAC10-1245, 35s::pTAC10-1467, and 35s::pTAC10-1740 plasmids were introduced into *ptac10-1* mutants, respectively. However, introduction of these truncated transgenes did not recover *ptac10-1* phenotype while introduction of the full-length *pTAC10* into the mutants was able to rescue the phenotype. These demonstrated that the intact C-terminal region of pTAC10 is essential for the pTAC10-PAP interactions to perform its function as a PEP subunit.

Since the C-terminal region is responsible for the pTAC10-PAP interactions, introducing a DNA construct overexpressing the C-terminal truncated *pTAC10* into Col-0 could cause a dominant negative effect on chloroplast development due to interfered interactions between endogenous pTAC10 and PAP. The results showed that the transgenic plants overexpressing *pTAC10-1467*, and *pTAC10-1740* in Col-0 background showed

abnormal whitening phenotype that was not observed in the wild-type or the full-length *pTAC10*-overexpressing plants. The structure of plastids in the whitened tissue was severely compromised compared to that in the green tissue even in the same transgenic plant. Morphology of plastids in the white tissue did not have the proper stacking of thylakoid membrane which was observed in the normal green tissues. Although the morphology of white and green tissues was totally different, the expression level of endogenous *pTAC10* was similar between the whitening-occurred and whitening-not-occurred transgenic plants or between whitened and green parts of the leaves in whitening-occurred plants. These findings indicate that the whitening phenotype might not be induced by endogenous or transgenic *pTAC10*. Rather, this whitening phenotype might be caused by the competition between the truncated pTAC10 and endogenous pTAC10 for the interaction with other PAPs, resulting in disturbed assembly of the PEP complex. In addition, compared to the *35s::pTAC10* transgenic plants, randomly whitened phenotype caused by overexpressing truncated *pTAC10*s imply that the protein compositions of the PEP complex might influence plastid signaling and development.

The analysis on *35s::pTAC10* transgenic plants demonstrated that overexpression of *pTAC10* promotes the PEP-dependent gene expression, chlorophyll contents, chloroplast development, and even plant growth. These phenotypes were not observed in plants overexpressing another *PAP*, *FSD3*. These differences suggested that pTAC10 functions as a key bottleneck for the establishment of the PEP complex through interacting with a wide range of PAPs. In addition, previous studies reported the protein compositions of PEP complex become more complicated as the development of plastids progressed from etioplasts to mature chloroplasts (Hu and Bogorad, 1990 ; Pfannschmidt and Link, 1997; Pfannschmidt et al., 2000). Despite studies compositional changes of PEP complex during chloroplast development, it still remains largely unknown when the PEP complex become functional during plant development. In this study, it was revealed that *pTAC10* is mainly expressed in the light-exposed tissues like leaves and its expression level is correlated to

chloroplast development. Expression of *pTAC10* also gradually rises as leaves mature and drastically decreases at leaf senescing stage. Moreover, *pTAC10*-overexpressing plants showed a tendency of higher PEP-dependent gene expression level, higher chlorophyll contents, and more chloroplasts per cell than the wild type. Collectively, these suggest that pTAC10 provides a broad range of interactions with PAPs, which enables pTAC10 to play a pivotal role in forming a PEP complex.

Overexpressing the full-length *pTAC10* gives rise to enhanced plant growth and productivity in *Arabidopsis*. These data gave a clue that plant growth and productivity could be regulated by chloroplast development. Further investigation of the functions of pTAC10 in PEP complex formation will help us to improve our understanding of mechanisms underlying chloroplasts development and inform strategies for creating transgenic crops with high yields.

References

Abdallah F, Salamini F and Leister D (2000) A prediction of the size and evolutionary origin of the proteome of chloroplasts of Arabidopsis, *Trends in Plant Science* 5(4), 141-142.

Akama K, Shiraishi H, Ohta S, Nakamura K, Okada K and Shimura Y (1992) Efficient transformation of Arabidopsis thaliana: comparison of the efficiencies with various organs, plant ecotypes and Agrobacterium strains, *Plant cell reports* 12(1), 7-11.

Allison L, Simon L and Maliga P (1996) Deletion of rpoB reveals a second distinct transcription system in plastids of higher plants, *The EMBO Journal* 15(11), 2802.

Arsova B, Hoja U, Wimmelbacher M, Greiner E, Þstün Ş, Melzer M et al. (2010) Plastidial thioredoxin z interacts with two fructokinase-like proteins in a thiol-dependent manner: evidence for an essential role in chloroplast development in Arabidopsis and Nicotiana benthamiana, *The Plant Cell* 22(5), 1498-1515.

Börner T, Aleynikova AY, Zubo YO and Kusnetsov VV (2015) Chloroplast RNA polymerases: Role in chloroplast biogenesis, *Biochimica et Biophysica Acta (BBA)-Bioenergetics* 1847(9), 761-769.

Bottomley W, Smith HJ and Bogorad L (1971) RNA polymerases of maize: partial purification and properties of the chloroplast enzyme, *Proceedings of the National Academy of Sciences* 68(10), 2412-2416.

Bradley D and Gatenby A (1985) Mutational analysis of the maize chloroplast ATPase-beta subunit gene promoter: the isolation of promoter mutants in E. coli and their characterization in a chloroplast in vitro transcription system, *The EMBO Journal* 4(13B), 3641-3648.

Briat JF, Laulhere JP and Mache R (1979) Transcription Activity of a DNA-Protein Complex Isolated from Spinach Plastids, *The FEBS Journal* 98(1), 285-292.

Bülow S, Reiss T and Link G (1987) DNA-binding proteins of the transcriptionally active chromosome from mustard (Sinapis alba L.) chloroplasts, *Current genetics* 12(2), 157-159.

Chen M, Galvão RM, Li M, Burger B, Bugea J, Bolado J et al. (2010) Arabidopsis HEMERA/pTAC12 initiates photomorphogenesis by phytochromes, *Cell* 141(7), 1230-1240.

Clough SJ and Bent AF (1998) Floral dip: a simplified method forAgrobacterium-mediated

transformation ofArabidopsis thaliana, *The Plant Journal* 16(6), 735-743.

Dubin MJ, Bowler C and Benvenuto G (2008) A modified Gateway cloning strategy for overexpressing tagged proteins in plants, *Plant Methods* 4(1), 3.

Emanuel C, Weihe A, Graner A, Hess WR and Börner T (2004) Chloroplast development affects expression of phage-type RNA polymerases in barley leaves, *The Plant Journal* 38(3), 460-472.

Eshed Y, Izhaki A, Baum SF, Floyd SK and Bowman JL (2004) Asymmetric leaf development and blade expansion in Arabidopsis are mediated by KANADI and YABBY activities, *Development* 131(12), 2997-3006.

Fleischmann TT, Scharff LB, Alkatib S, Hasdorf S, Schöttler MA and Bock R (2011) Nonessential plastid-encoded ribosomal proteins in tobacco: a developmental role for plastid translation and implications for reductive genome evolution, *The Plant Cell* 23(9), 3137-3155.

Gao ZP, Yu QB, Zhao TT, Ma Q, Chen GX and Yang Z-N (2011) A functional component of the transcriptionally active chromosome complex, Arabidopsis pTAC14, interacts with pTAC12/HEMERA and regulates plastid gene expression, *Plant physiology* 157(4), 1733-1745.

Garcia M, Myouga F, Takechi K, Sato H, Nabeshima K, Nagata N et al. (2008) An Arabidopsis homolog of the bacterial peptidoglycan synthesis enzyme MurE has an essential role in chloroplast development, *The Plant Journal* 53(6), 924-934.

Gilkerson J, Perez-Ruiz JM, Chory J and Callis J (2012) The plastid-localized pfkB-type carbohydrate kinases FRUCTOKINASE-LIKE 1 and 2 are essential for growth and development of Arabidopsis thaliana, *BMC plant biology* 12(1), 102.

Hajdukiewicz PT, Allison LA and Maliga P (1997) The two RNA polymerases encoded by the nuclear and the plastid compartments transcribe distinct groups of genes in tobacco plastids, *The EMBO Journal* 16(13), 4041-4048.

Hallick RB, Lipper C, Richards OC and Rutter WJ (1976) Isolation of a transcriptionally active chromosome from chloroplasts of Euglena gracilis, *Biochemistry* 15(14), 3039-3045.

Hess W, Prombona A, Fieder B, Subramanian A and Börner T (1993) Chloroplast rps15 and the rpoB/C1/C2 gene cluster are strongly transcribed in ribosome-deficient plastids: evidence for a functioning non-chloroplast-encoded RNA polymerase, *The EMBO Journal* 12(2), 563-571.

Holsters M, De Waele D, Depicker A, Messens E, Van Montagu M and Schell J (1978) Transfection and transformation of Agrobacterium tumefaciens, *Molecular and General Genetics MGG*

163(2), 181-187.

Hu J and Bogorad L (1990) Maize chloroplast RNA polymerase: the 180-, 120-, and 38-kilodalton polypeptides are encoded in chloroplast genes, *Proceedings of the National Academy of Sciences* 87(4), 1531-1535.

Huang C, Yu QB, Lv R-H, Yin QQ, Chen GY, Xu L et al. (2013) The reduced plastid-encoded polymerase-dependent plastid gene expression leads to the delayed greening of the Arabidopsis fln2 mutant, *PloS one* 8(9), e73092.

Husbands AY, Benkovics AH, Nogueira FT, Lodha M and Timmermans MC (2015) The ASYMMETRIC LEAVES complex employs multiple modes of regulation to affect adaxial-abaxial patterning and leaf complexity, *The Plant Cell* 27(12), 3321-3335.

Iwakawa H, Iwasaki M, Kojima S, Ueno Y, Soma T, Tanaka H et al. (2007) Expression of the ASYMMETRIC LEAVES2 gene in the adaxial domain of Arabidopsis leaves represses cell proliferation in this domain and is critical for the development of properly expanded leaves, *The Plant Journal* 51(2), 173-184.

Jeon Y, Jung HJ, Kang H, Park YI, Lee SH and Pai HS (2012) S1 domain-containing STF modulates plastid transcription and chloroplast biogenesis in Nicotiana benthamiana, *New Phytologist* 193(2), 349-363.

Kapoor S, Suzuki JY and Sugiura M (1997) Identification and functional significance of a new class of non-consensus-type plastid promoters, *The Plant Journal* 11(2), 327-337.

Kerstetter RA, Bollman K, Taylor RA, Bomblies K and Poethig RS (2001) KANADI regulates organ polarity in Arabidopsis, *Nature* 411(6838), 706.

Kindgren P and Strand Ç (2015) Chloroplast transcription, untangling the Gordian Knot, *New Phytologist* 206(3), 889-891.

Krause K and Krupinska K (2000) Molecular and functional properties of highly purified transcriptionally active chromosomes from spinach chloroplasts, *Physiologia plantarum* 109(2), 188-195.

Krause K, Maier R, Kofer W, Krupinska K and Herrmann R (2000) Disruption of plastid-encoded RNA polymerase genes in tobacco: expression of only a distinct set of genes is not based on selective transcription of the plastid chromosome, *Molecular and General Genetics MGG* 263(6), 1022-1030.

Krupinska K, Melonek J and Krause K (2013) New insights into plastid nucleoid structure and functionality, *Planta* 237(3), 653-664.

Legen J, Kemp S, Krause K, Profanter B, Herrmann RG and Maier RM (2002) Comparative analysis of plastid transcription profiles of entire plastid chromosomes from tobacco attributed to wild-type and PEP-deficient transcription machineries, *The Plant Journal* 31(2), 171-188.

Lerbs S, Bräutigam E and Parthier B (1985) Polypeptides of DNA-dependent RNA polymerase of spinach chloroplasts: characterization by antibody-linked polymerase assay and determination of sites of synthesis, *The EMBO Journal* 4(7), 1661-1666.

Lgloi G and Kössel H (1992) The transcriptional apparatus of chloroplasts, *Critical reviews in plant sciences* 10(6), 525-558.

Lin W-C, Shuai B and Springer PS (2003) The Arabidopsis LATERAL ORGAN BOUNDARIES–domain gene ASYMMETRIC LEAVES2 functions in the repression of KNOX gene expression and in adaxial-abaxial patterning, *The Plant Cell* 15(10), 2241-2252.

Little MC and Hallick R (1988) Chloroplast rpoA, rpoB, and rpoC genes specify at least three components of a chloroplast DNA-dependent RNA polymerase active in tRNA and mRNA transcription, *Journal of Biological Chemistry* 263(28), 14302-14307.

Llave C, Kasschau KD and Carrington JC (2000) Virus-encoded suppressor of posttranscriptional gene silencing targets a maintenance step in the silencing pathway, *Proceedings of the National Academy of Sciences* 97(24), 13401-13406.

Loschelder H, Homann A, Ogrzewalla K and Link G (2004) Proteomics-based sequence analysis of plant gene expression–the chloroplast transcription apparatus, *Phytochemistry* 65(12), 1785-1793.

Machida C, Nakagawa A, Kojima S, Takahashi H and Machida Y (2015) The complex of ASYMMETRIC LEAVES (AS) proteins plays a central role in antagonistic interactions of genes for leaf polarity specification in Arabidopsis, *Wiley Interdisciplinary Reviews: Developmental Biology* 4(6), 655-671.

Majeran W, Friso G, Asakura Y, Qu X, Huang M, Ponnala L et al. (2011) Nucleoid-enriched proteomes in developing plastids and chloroplasts from maize leaves; a new conceptual framework for nucleoid functions, *Plant physiology*, pp. 111.188474.

Martin W, Rujan T, Richly E, Hansen A, Cornelsen S, Lins T et al. (2002) Evolutionary analysis of

Arabidopsis, cyanobacterial, and chloroplast genomes reveals plastid phylogeny and thousands of cyanobacterial genes in the nucleus, *Proceedings of the National Academy of Sciences* 99(19), 12246-12251.

Mateo-Bonmatí E, Casanova-Sáez R, Quesada V, Hricová A, Candela H and Micol JL (2015) Plastid control of abaxial-adaxial patterning, *Scientific Reports* 5, 15975.

Matsumura Y, Ohbayashi I, Takahashi H, Kojima S, Ishibashi N, Keta S et al. (2016) A genetic link between epigenetic repressor AS1-AS2 and a putative small subunit processome in leaf polarity establishment of Arabidopsis, *Biology open*, bio. 019109.

Melonek J, Matros A, Trösch M, Mock H-P and Krupinska K (2012) The core of chloroplast nucleoids contains architectural SWIB domain proteins, *The Plant Cell* 24(7), 3060-3073.

Moschopoulos A, Derbyshire P and Byrne ME (2012) The Arabidopsis organelle-localized glycyl-tRNA synthetase encoded by EMBRYO DEFECTIVE DEVELOPMENT1 is required for organ patterning, *Journal of experimental botany* 63(14), 5233-5243.

Motohashi R, Nagata N, Ito T, Takahashi S, Hobo T, Yoshida S et al. (2001) An essential role of a TatC homologue of a ΔpH-dependent protein transporter in thylakoid membrane formation during chloroplast development in Arabidopsis thaliana, *Proceedings of the National Academy of Sciences* 98(18), 10499-10504.

Myouga F, Hosoda C, Umezawa T, Iizumi H, Kuromori T, Motohashi R et al. (2008) A heterocomplex of iron superoxide dismutases defends chloroplast nucleoids against oxidative stress and is essential for chloroplast development in Arabidopsis, *The Plant Cell* 20(11), 3148-3162.

Newcomb W (1986) An Introduction to Plant Cell Development. Jeremy Burgess, *The Quarterly Review of Biology* 61(4), 535-535.

Pekker I, Alvarez JP and Eshed Y (2005) Auxin response factors mediate Arabidopsis organ asymmetry via modulation of KANADI activity, *The Plant Cell* 17(11), 2899-2910.

Peltier JB, Cai Y, Sun Q, Zabrouskov V, Giacomelli L, Rudella A et al. (2006) The oligomeric stromal proteome of Arabidopsis thaliana chloroplasts, *Molecular & Cellular Proteomics* 5(1), 114-133.

Pfalz J, Holtzegel U, Barkan A, Weisheit W, Mittag M and Pfannschmidt T (2015) ZmpTAC12 binds single-stranded nucleic acids and is essential for accumulation of the plastid-encoded

polymerase complex in maize, *New Phytologist* 206(3), 1024-1037.

Pfalz J, Liere K, Kandlbinder A, Dietz K-J and Oelmüller R (2006) pTAC2,-6, and-12 are components of the transcriptionally active plastid chromosome that are required for plastid gene expression, *The Plant Cell* 18(1), 176-197.

Pfalz J and Pfannschmidt T (2013) Essential nucleoid proteins in early chloroplast development, *Trends in Plant Science* 18(4), 186-194.

Pfannschmidt T, Blanvillain R, Merendino L, Courtois F, Chevalier F, Liebers M et al. (2015) Plastid RNA polymerases: orchestration of enzymes with different evolutionary origins controls chloroplast biogenesis during the plant life cycle, *Journal of experimental botany* 66(22), 6957-6973.

Pfannschmidt T and Link G (1994) Separation of two classes of plastid DNA-dependent RNA polymerases that are differentially expressed in mustard (Sinapis alba L.) seedlings, *Plant molecular biology* 25(1), 69-81.

Pfannschmidt T and Link G (1997) The A and B forms of plastid DNA-dependent RNA polymerase from mustard (Sinapis alba L.) transcribe the same genes in a different developmental context, *Molecular and General Genetics MGG* 257(1), 35-44.

Pfannschmidt T, Ogrzewalla K, Baginsky S, Sickmann A, Meyer HE and Link G (2000) The multisubunit chloroplast RNA polymerase A from mustard (Sinapis alba L.), *The FEBS Journal* 267(1), 253-261.

Puthiyaveetil S, Ibrahim IM, Jeličić B, Tomašić A, Fulgosi H and Allen JF (2010) Transcriptional control of photosynthesis genes: the evolutionarily conserved regulatory mechanism in plastid genome function, *Genome biology and evolution* 2, 888-896.

Rajasekhar VK, Sun E, Meeker R, Wu BW and Tewari KK (1991) Highly purified pea chloroplast RNA polymerase transcribes both rRNA and mRNA genes, *The FEBS Journal* 195(1), 215-228.

Ravanel S, Gakière B, Job D and Douce R (1998) The specific features of methionine biosynthesis and metabolism in plants, *Proceedings of the National Academy of Sciences* 95(13), 7805-7812.

Rawsthorne S (2002) Carbon flux and fatty acid synthesis in plants, *Progress in lipid research* 41(2), 182-196.

Reiss T and Link G (1985) Characterization of transcriptionally active DNA-protein complexes from chloroplasts and etioplasts of mustard (Sinapis alba L.), *The FEBS Journal* 148(2), 207-

212.

Ristic Z, Momčilović I, Fu J, Callegari E and Deridder BP (2007) Chloroplast protein synthesis elongation factor, EF-Tu, reduces thermal aggregation of rubisco activase, *Journal of Plant Physiology* 164(12), 1564-1571.

Saeed AI, Bhagabati NK, Braisted JC, Liang W, Sharov V, Howe EA et al. (2006) [9] TM4 microarray software suite, *Methods in enzymology* 411, 134-193.

Sagan L (1967) On the origin of mitosing cells, *Journal of theoretical biology* 14(3), 225-IN226.

Sakai A, Saito C, Inada N and Kuroiwa T (1998) Transcriptional activities of the chloroplast-nuclei and proplastid-nuclei isolated from tobacco exhibit different sensitivities to tagetitoxin: implication of the presence of distinct RNA polymerases, *Plant and Cell Physiology* 39(9), 928-934.

Santis-Maciossek D, Kofer W, Bock A, Schoch S, Maier RM, Wanner G et al. (1999) Targeted disruption of the plastid RNA polymerase genes rpoA, B and C1: molecular biology, biochemistry and ultrastructure, *The Plant Journal* 18(5), 477-489.

Schröter Y, Steiner S, Matthäi K and Pfannschmidt T (2010) Analysis of oligomeric protein complexes in the chloroplast sub-proteome of nucleic acid-binding proteins from mustard reveals potential redox regulators of plastid gene expression, *Proteomics* 10(11), 2191-2204.

Serrano I, Audran C and Rivas S (2016) Chloroplasts at work during plant innate immunity, *Journal of experimental botany* 67(13), 3845-3854.

Siegfried KR, Eshed Y, Baum SF, Otsuga D, Drews GN and Bowman JL (1999) Members of the YABBY gene family specify abaxial cell fate in Arabidopsis, *Development* 126(18), 4117-4128.

Soll J and Schleiff E (2004) Protein import into chloroplasts, *Nature reviews Molecular cell biology* 5(3), 198.

Steiner S, Schröter Y, Pfalz J and Pfannschmidt T (2011) Identification of essential subunits in the plastid-encoded RNA polymerase complex reveals building blocks for proper plastid development, *Plant physiology* 157(3), 1043-1055.

Sumanta N, Haque CI, Nishika J and Suprakash R (2014) Spectrophotometric analysis of chlorophylls and carotenoids from commonly grown fern species by using various extracting solvents, *Research Journal of Chemical Sciences* 4(9), 63-69.

Thole V, Alves SC, Worland B, Bevan MW and Vain P (2009) A protocol for efficiently retrieving

and characterizing flanking sequence tags (FSTs) in Brachypodium distachyon T-DNA insertional mutants, *Nature protocols* 4(5), 650.

Wicke S, Schneeweiss GM, Müller KF and Quandt D (2011) The evolution of the plastid chromosome in land plants: gene content, gene order, gene function, *Plant molecular biology* 76(3-5), 273-297.

Williams-Carrier R, Zoschke R, Belcher S, Pfalz J and Barkan A (2014) A major role for the plastid-encoded RNA polymerase complex in the expression of plastid transfer RNAs, *Plant physiology* 164(1), 239-248.

Wimmelbacher M and Börnke F (2014) Redox activity of thioredoxin z and fructokinase-like protein 1 is dispensable for autotrophic growth of Arabidopsis thaliana, *Journal of experimental botany* 65(9), 2405-2413.

Yagi Y, Ishizaki Y, Nakahira Y, Tozawa Y and Shiina T (2012) Eukaryotic-type plastid nucleoid protein pTAC3 is essential for transcription by the bacterial-type plastid RNA polymerase, *Proceedings of the National Academy of Sciences* 109(19), 7541-7546.

Yagi Y and Shiina T (2014) Recent advances in the study of chloroplast gene expression and its evolution, *Frontiers in plant science* 5, 61.

Yu QB, Huang C and Yang ZN (2014) Nuclear-encoded factors associated with the chloroplast transcription machinery of higher plants, *Frontiers in plant science* 5.

Yu QB, Zhao TT, Ye LS, Cheng L, Wu YQ, Huang C et al. (2018) pTAC10, an S1-domain-containing component of the transcriptionally active chromosome complex, is essential for plastid gene expression in Arabidopsis thaliana and is phosphorylated by chloroplast-targeted casein kinase II, *Photosynthesis Research*, 1-15.

Yu QB, Lu Y, Ma Q, Zhao TT, Huang C, Zhao HF et al. (2013) TAC7, an essential component of the plastid transcriptionally active chromosome complex, interacts with FLN1, TAC10, TAC12 and TAC14 to regulate chloroplast gene expression in Arabidopsis thaliana, *Physiologia plantarum* 148(3), 408-421.

Zhang X, Garreton V and Chua NH (2005) The AIP2 E3 ligase acts as a novel negative regulator of ABA signaling by promoting ABI3 degradation, *Genes & Development* 19(13), 1532-1543.

Zhelyazkova P, Sharma CM, Förstner KU, Liere K, Vogel J and Börner T (2012) The primary transcriptome of barley chloroplasts: numerous noncoding RNAs and the dominating role of the

plastid-encoded RNA polymerase, *The Plant Cell* 24(1), 123-136.

Parameter	Plant		Average	SD	Δ%	*P*
Height (mm)	Wild type	Col-0	294.82	24.49	-	-
	35s:: pTAC10	Line 1	298.00	27.57	1.079	0.778
		Line 2	284.00	19.27	-3.669	0.264
		Line 3	297.73	26.61	0.987	0.792
Dry weight (g)	Wild type	Col-0	1.653	0.230	-	-
	35s:: pTAC10	Line 1	2.090	0.339	26.437	0.002
		Line 2	1.960	0.230	18.561	0.005
		Line 3	1.897	0.229	14.745	0.021
Total seed weight (g)	Wild type	Col-0	0.080	0.013	-	-
	35s:: pTAC10	Line 1	0.097	0.015	21.178	0.010
		Line 2	0.093	0.013	16.421	0.027
		Line 3	0.089	0.009	11.438	0.073

Table 1. Biomass and productivity of *pTAC10*-overexpressing transgenic plants.

The height, dry weight and total seed weight of *35s::pTAC10* transgenic plants were measured to analyze their biomass and productivity. The transgenic and wild-type plants were grown under the same conditions for 4 months (n > 10). Each transgenic line was independent and the measurement was repeated twice with similar results.

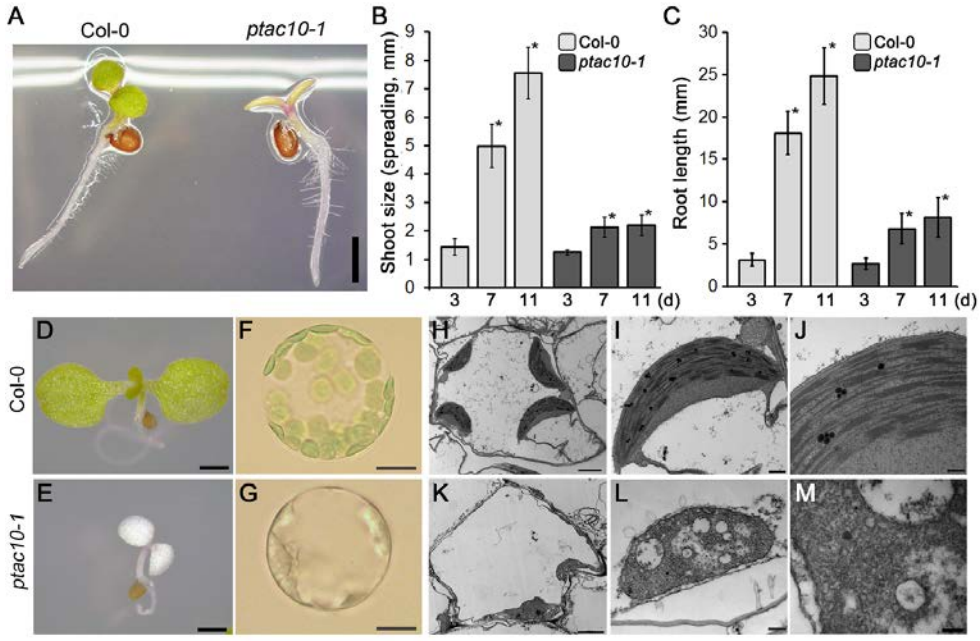
A
Col-0
ptac10-1
B
Shoot size (spreading, mm)
Col-0
ptac10-1
3 7 11 3 7 11 (d)
C
Root length (mm)
Col-0
ptac10-1
3 7 11 3 7 11 (d)
D
F
H
I
J
Col-0
E
G
K
L
M
ptac10-1

Figure 1. Characterization of *ptac10-1* mutants with defects in chloroplast development.

(**A**) Photograph showing Col-0 and *ptac10-1* mutant seedlings grown in half-strength MS medium for 3 days. (**B** and **C**) Growth dynamics of the shoot (B) and root (C) from 3, 7 and 11 days after germination. Error bars represent SD. Statistical comparison was done by Student's *t*-test for each time point separately, and asterisks indicate statistically significant differences between the conditions (*p*-value < 0.01, *t*-test). (**D**-**E**) Images of 7-day-old Col-0 (D) and *ptac10-1* mutant (E) seedlings. Scale bar = 1 mm. (**F**-**G**) Images of protoplasts isolated from 7-day-old Col-0 (F) and *ptac10-1* mutant (G) seedlings. Scale bar = 5 μm. (**H**-**M**) Ultrastructure of chloroplasts in Col-0 (H-J) and *ptac10-1* mutants (K-M). Scale bars = 2 μm (left), 500 nm (middle) and 200 nm (right).

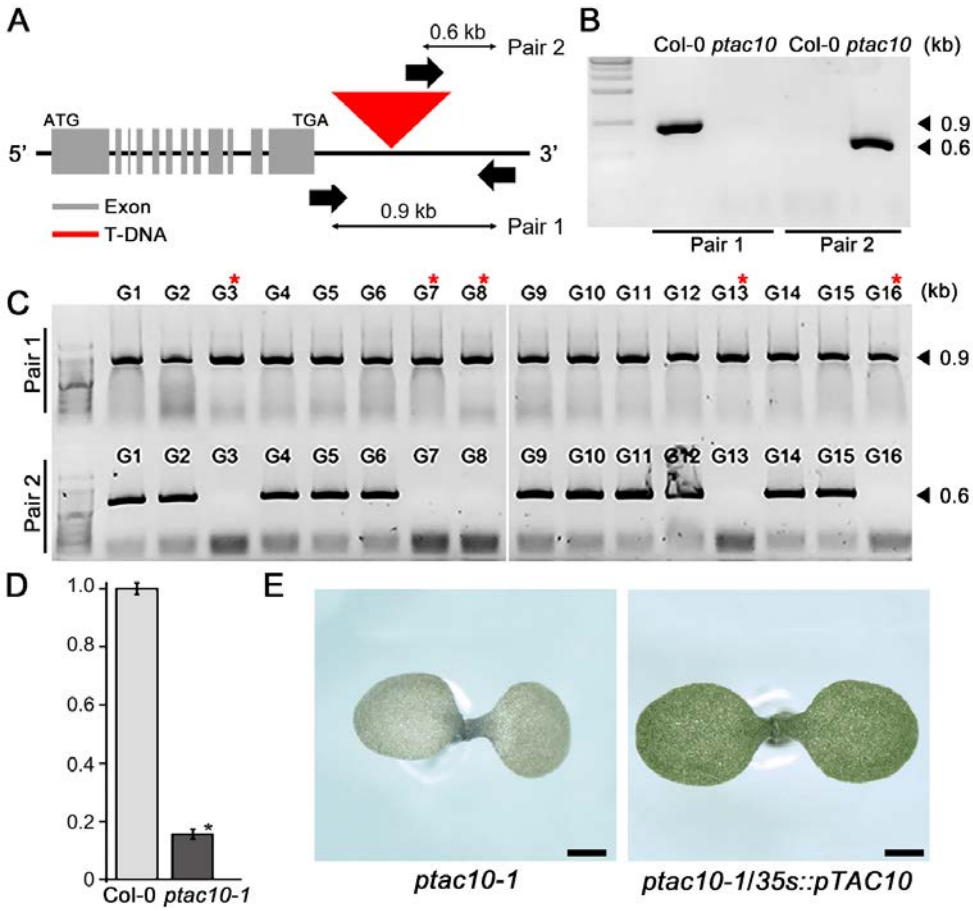
A
0.6 kb
Pair 2
ATG
TGA
5'
3'
Exon
T-DNA
0.9 kb
Pair 1
B
Col-0 ptac10 Col-0 ptac10 (kb)
0.9
0.6
Pair 1
Pair 2
C
G1 G2 G3* G4 G5 G6 G7* G8* G9 G10 G11 G12 G13* G14 G15 G16* (kb)
Pair 1
Pair 2
0.9
0.6
D
1.0
0.8
0.6
0.4
0.2
0
Col-0 ptac10-1
E
ptac10-1
ptac10-1/35s::pTAC10

Figure 2. The T-DNA insertion allele of *pTAC10* used in this study and its genotyping. (**A**) Graphical depiction of *pTAC10* gene structure and location of T-DNA insertion in the *ptac10-1* allele. Grey boxes, red triangle and black arrows indicate exons of *pTAC10*, inserted T-DNA, and the primers used for PCR-based genotyping, respectively. (**B**) PCR-based genotyping results of the homozygous *ptac10-1* mutant. Genomic DNA of Col-0 and homozygous *ptac10-1* mutant and two sets of primers called primer pair 1 (0.9 kb; left 2 lanes) or primer pair 2 (0.6 kb; right 2 lanes) as indicated in (A) were used for the assay. *ptac10* indicates the homozygous *ptac10-1* allele (**C**) PCR-based genotyping of 16 seedlings with green leaves (G1 to G16) obtained from self-pollinated *ptac10-1* heterozygous mutants. Red asterisks indicate the homozygous wild-type (+/+) for the T-DNA insertion and the others are the heterozygous mutant plants (+/-). (**D**) Expression analysis of *pTAC10* in Col-0 and *ptac10-1* homozygous mutants by qRT-PCR. Error bars indicated SD. The asterisk indicates a statistically significant difference between *ptac10-1* and Col-0 (p-value < 0.01, t-test). (**E**) Complementation assay of *ptac10-1* mutant. The introduction of cDNA of the full-length *pTAC10* recovered the *ptac10-1* mutant phenotype. Scale bars = 1 mm.

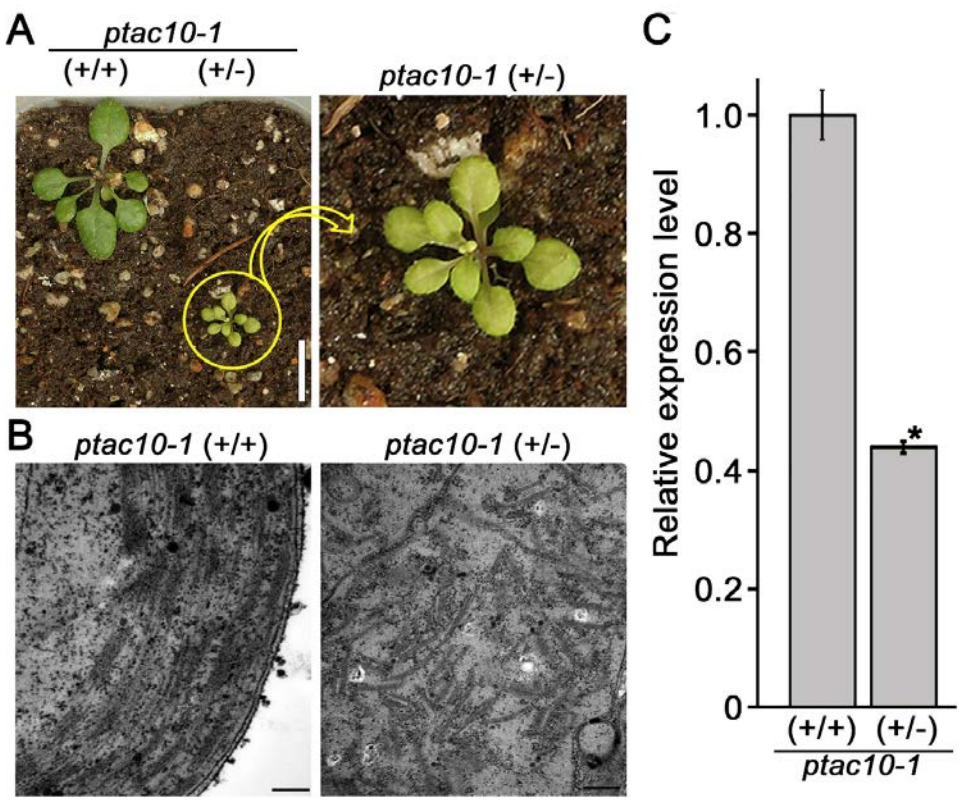
A
ptac10-1
(+/+)
(+/-)
ptac10-1 (+/-)
B
ptac10-1 (+/+)
ptac10-1 (+/-)
C
Relative expression level
1.0
0.8
0.6
0.4
0.2
0
*
(+/+)
(+/-)
ptac10-1

Figure 3. The phenotype of heterozygous *ptac10-1* mutants.

(**A**) Images of 3-week-old wild-type (+/+; left) and *ptac10-1* heterozygous mutant (+/-; right) plants. Scale bar = 1 cm. (**B**) Ultrastructure of chloroplasts in wild-type (+/+; left) and heterozygous *ptac10-1* mutant (+/-; right) was observed by TEM. Scale bar = 200 nm. (**C**) Expression level of *pTAC10* in the wild type (+/+) and heterozygous *ptac10-1* mutant (+/-) by qRT-PCR. Error bars indicated SD. The asterisk indicates a statistically significant difference between the heterozygous *ptac10-1* mutants and wild-type plants (*p*-value < 0.01, *t*-test).

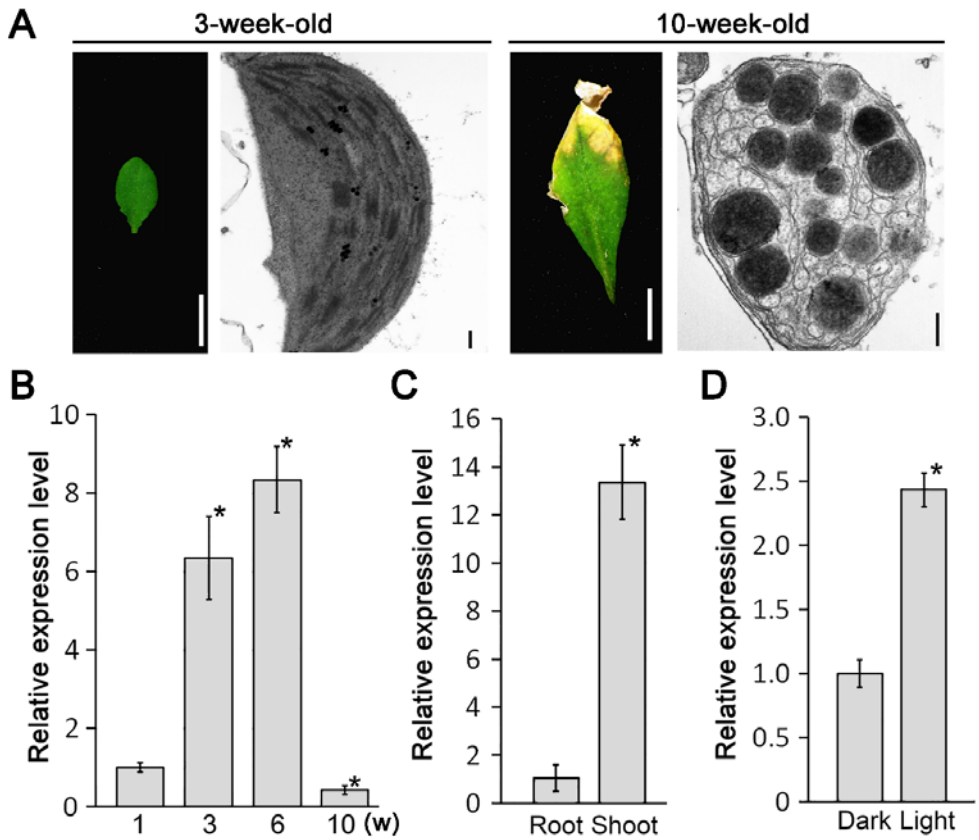
A
3-week-old
10-week-old
B
Relative expression level
10
8
6
4
2
0
1
3
6
10 (w)
C
Relative expression level
16
14
12
10
8
6
4
2
0
Root Shoot
D
Relative expression level
3.0
2.5
2.0
1.5
1.0
0.5
0
Dark Light

Figure 4. Changes in the expression pattern of *pTAC10* during leaf development.

(**A**) A leaf morphology and ultrastructure of chloroplast in 3-week-old and 10-week-old Col-0 plants. Scale bar = 5 mm in leaf images and 200 nm in chloroplast images. (**B**) qRT-PCR analysis of *pTAC10* expression level at the indicated stages. RNA was extracted from cotyledons of 1-week-old seedlings and seventh or eighth rosette leaves of 3-, 6-, or 10-week-old Col-0 plants. (**C**) qRT-PCR analysis of *pTAC10* expression in the root and shoot of 1-week-old Col-0 plants. (**D**) Relative expression of *pTAC10* was analyzed in 1-week-old Col-0 seedlings grown at the continuous dark or light conditions. Error bars indicate SD. The asterisks indicate a statistically significant difference between the corresponding samples and their controls (p-value < 0.01, t-test).

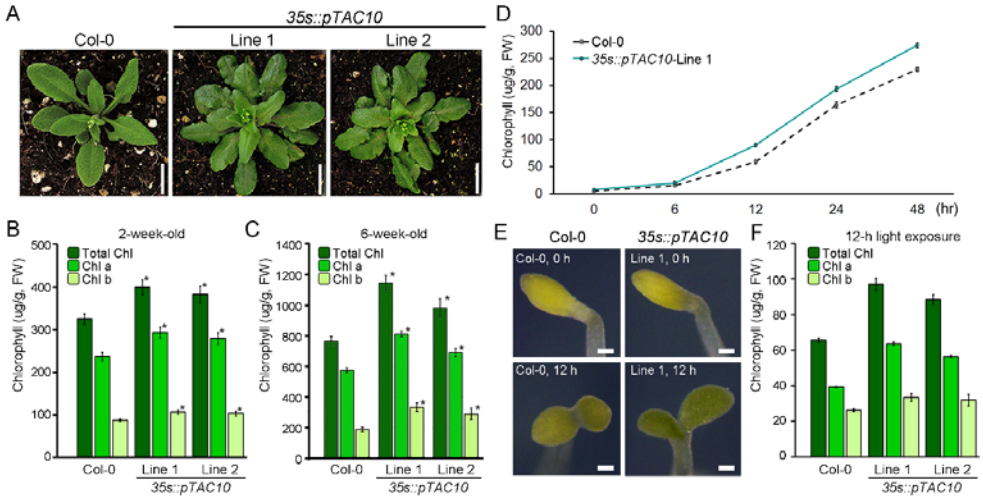
A
35s::pTAC10
Col-0
Line 1
Line 2
D
Col-0
35s::pTAC10-Line 1
Chlorophyll (ug/g. FW)
0
6
12
24
48 (hr)
B
2-week-old
Total Chl
Chl a
Chl b
Chlorophyll (ug/g. FW)
Col-0
Line 1
Line 2
35s::pTAC10
C
6-week-old
E
Col-0
35s::pTAC10
Col-0, 0 h
Line 1, 0 h
Col-0, 12 h
Line 1, 12 h
F
12-h light exposure

Figure 5. Overexpression of *pTAC10* influences plant leaf greening.

(**A**) Morphology of 2 independent lines of the *pTAC10*-overexpressing transgenic plants and Col-0 plants grown for 5 weeks in soil. Scale bars = 1 cm. (**B** and **C**) Quantification of chlorophyll contents in 2-week-old (B) and 6-week-old (C) *35s::pTAC10* and Col-0. (**D**) Graph showing the changes in chlorophyll contents in the etiolated seedlings of Col-0 and *pTAC10*-overexpressing plants after continuous light exposure. During de-etiolation, chlorophyll contents in these seedlings were measured at the indicated time. (**E**) Morphological change of *35s::pTAC10* and Col-0 during de-etiolation. Etiolated seedlings were exposed to light for the indicated time. Scale bar = 0.2 mm. (**F**) Chlorophyll contents of *35s::pTAC10* and Col-0 were quantified independently using etiolated seedlings exposed to continuous light for 12 hours. Error bars indicate SD. The asterisks indicate a statistically significant difference between the *pTAC10*-overexpressing plants and Col-0 (p-value < 0.01, t-test).

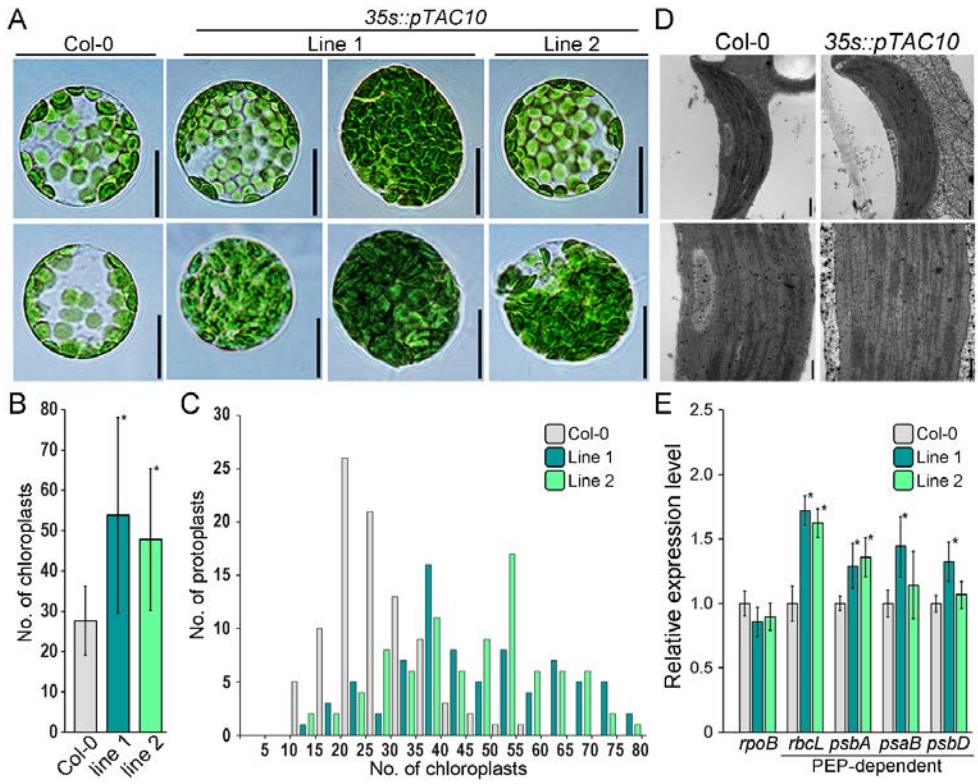
A
35s::pTAC10
Col-0
Line 1
Line 2
D
Col-0
35s::pTAC10
B
No. of chloroplasts
Col-0
line 1
line 2
C
No. of protoplasts
Col-0
Line 1
Line 2
No. of chloroplasts
E
Relative expression level
Col-0
Line 1
Line 2
rpoB
rbcL
psbA
psaB
psbD
PEP-dependent

Figure 6. Overexpression of *pTAC10* promotes chloroplast development and photosynthetic gene expression.

(**A**) Protoplasts isolated from 2 independent lines of *35s::pTAC10* (line 1 and 2) and Col-0 plants grown in soil for 6 weeks. Scale bars = 10 μm. (**B** and **C**) Quantification of the number of chloroplasts observed in protoplasts isolated from Col-0 and *pTAC10*-overexpressing plants. The average number of chloroplasts was displayed in (B) and the number of protoplasts containing the indicated number of chloroplasts was shown in (C). (**D**) Chloroplast ultrastructure of the *pTAC10*-overexpressing transgenic plants (line 1) and Col-0 grown under the same conditions for 6 weeks. Scale bar = 500 nm in the top images and 200 nm in the bottom images. (**E**) Expression level of chloroplast genes in 6-week-old *pTAC10*-overexpressing and wild-type plants. Error bars indicate SD. The asterisks indicate a statistically significant difference between the corresponding samples and their controls (p-value < 0.01, t-test).

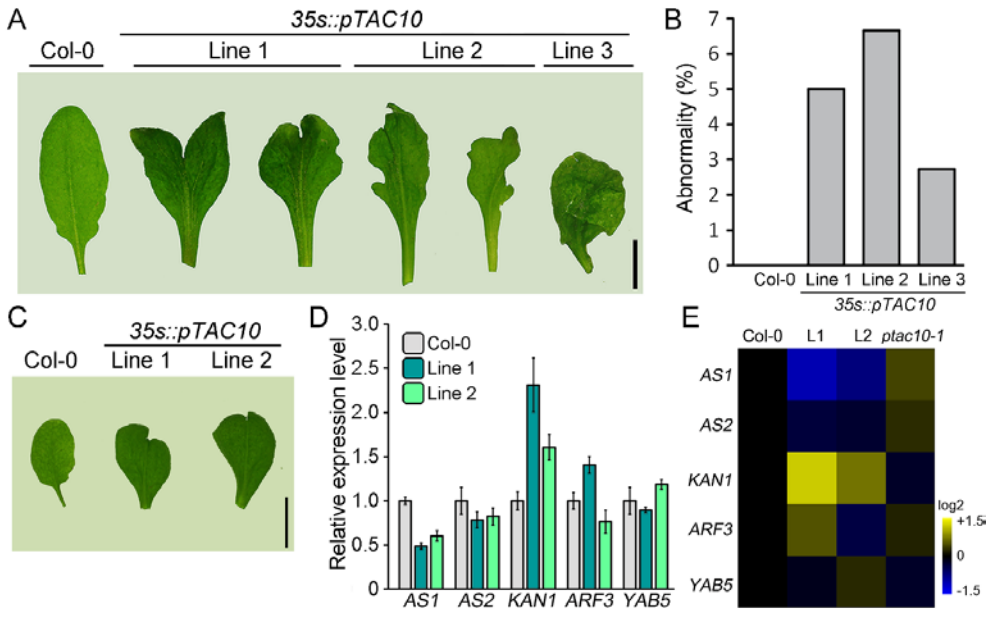
A
35s::pTAC10
Col-0
Line 1
Line 2
Line 3
B
Abnormality (%)
0
1
2
3
4
5
6
7
Col-0
Line 1
Line 2
Line 3
35s::pTAC10
C
35s::pTAC10
Col-0
Line 1
Line 2
D
Relative expression level
0
0.5
1.0
1.5
2.0
2.5
3.0
Col-0
Line 1
Line 2
AS1
AS2
KAN1
ARF3
YAB5
E
Col-0
L1
L2
ptac10-1
AS1
AS2
KAN1
ARF3
YAB5
log2
+1.5
0
-1.5

Figure 7. Overexpression of *pTAC10* induces abnormal leaf morphology.

(**A**) Images of leaves with abnormal morphology. The leaves were collected from 8-week-old *35s::pTAC10* transgenic plants. Scale bar = 1 cm. (**B**) Graph showing the ratio of abnormal leaves to normal leaves. (**C**) Images of abnormal leaves collected from 4-week-old *35s::pTAC10* transgenic plants. Scale bar = 1 cm. (**D**) qRT-PCR analysis showing the relative expression levels of the genes regulating leaf shape in the leaves with abnormal morphology (**E**) Heat map showing the expression patterns of the leaf shape-regulating genes in wild-type, *pTAC10*-overexpressing and *ptac10-1* mutant plants. Expression levels of these genes were obtained from qRT-PCR results (L1, L2 and Col-0) or RNA sequencing results (*ptac10-1*). L1 and L2 indicate the abnormal leaves collected from *pTAC10*-overexpressing transgenic plants line 1 (L1) and line 2 (L2).

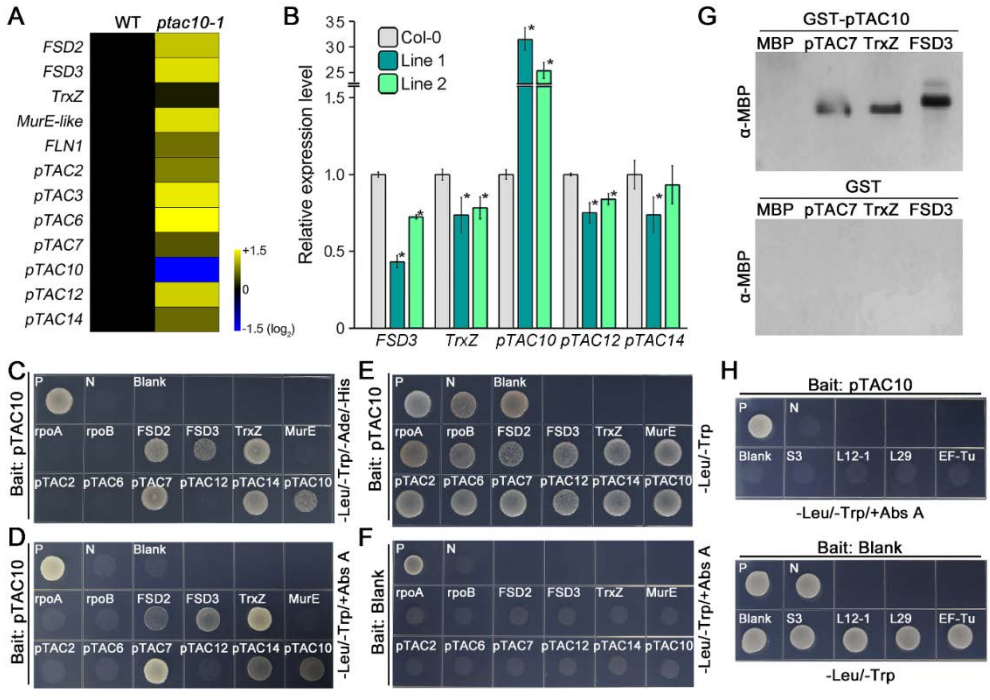
A
WT
ptac10-1
FSD2
FSD3
TrxZ
MurE-like
FLN1
pTAC2
pTAC3
pTAC6
pTAC7
pTAC10
pTAC12
pTAC14
+1.5
0
-1.5 (log2)
B
Relative expression level
Col-0
Line 1
Line 2
FSD3
TrxZ
pTAC10
pTAC12
pTAC14
G
GST-pTAC10
MBP pTAC7 TrxZ FSD3
α-MBP
GST
MBP pTAC7 TrxZ FSD3
α-MBP
C
Bait: pTAC10
-Leu/-Trp/-Ade/-His
P
N
Blank
rpoA
rpoB
FSD2
FSD3
TrxZ
MurE
pTAC2
pTAC6
pTAC7
pTAC12
pTAC14
pTAC10
D
Bait: pTAC10
-Leu/-Trp/+Abs A
E
Bait: pTAC10
-Leu/-Trp
F
Bait: Blank
-Leu/-Trp/+Abs A
H
Bait: pTAC10
S3
L12-1
L29
EF-Tu
-Leu/-Trp/+Abs A
Bait: Blank
-Leu/-Trp

Figure 8. Characterization of pTAC10 interaction with other PAPs.

(**A** and **B**) *PAP* expression pattern in *ptac10-1* and *pTAC10*-overexpressing transgenic plants compared to the wild-type. RNA sequencing results using 1-week-old *ptac10-1* and Col-0 seedlings were shown as a heat map (A) and qRT-PCR results using 6-week-old *35s::pTAC10* (line 1 and 2) and Col-0 plants were displayed as a bar graph (B). Error bars indicate SD. Asterisks indicate statistically significant differences between the corresponding samples and their control (p-value < 0.01, t-test). (**C**-**F**) Y2H assay showing the interaction between pTAC10 and subunits of PEP complex. The yeast lines were incubated on QDO medium (C) and Abs A-treated DDO medium (D) to test the interactions. DDO medium was used to validate yeast transformation and equal dropping (E). To check autoactivation of the prey plasmids, blank bait plasmid analysis was performed (F). P, N and blank indicate a positive control, a negative control and an autoactivation control, respectively. (**G**) GST pull-down assay showing that pTAC10 binds to other PAPs. MBP protein alone and GST protein alone were used as negative controls for the pTAC10-PAP interaction. (**H**) Y2H assay showing the interaction between pTAC10 and plastid translation machinery components.

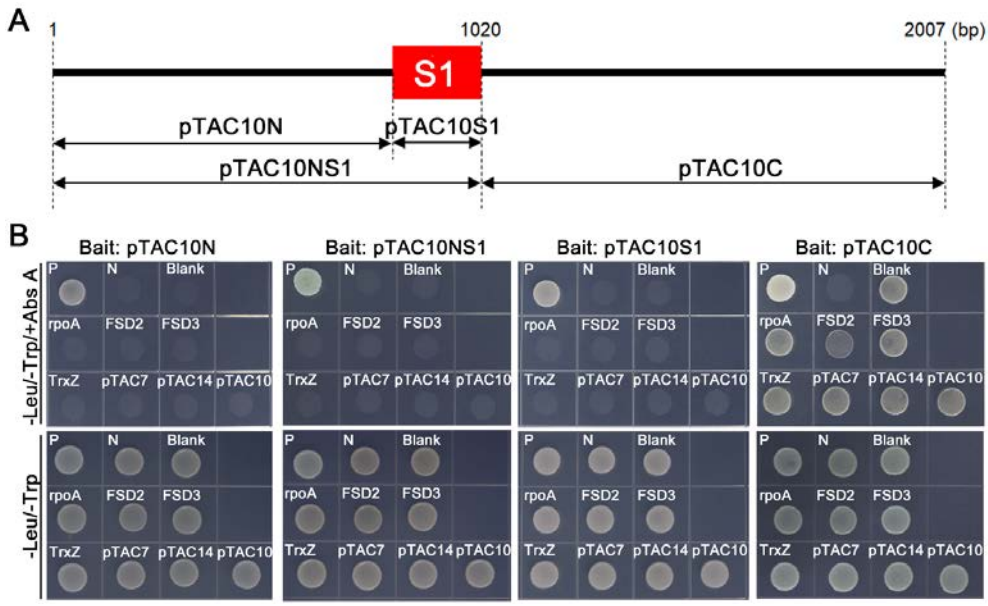
A
1
1020
2007 (bp)
S1
pTAC10N
pTAC10S1
pTAC10NS1
pTAC10C
B
Bait: pTAC10N
Bait: pTAC10NS1
Bait: pTAC10S1
Bait: pTAC10C
-Leu/-Trp/+Abs A
-Leu/-Trp
P
N
Blank
rpoA
FSD2
FSD3
TrxZ
pTAC7
pTAC14
pTAC10

Figure 9. The N-terminal region and S1 domain of pTAC10 are not involved in the pTAC10-PAP interactions.

(**A**) Simplified graphical depiction of *pTAC10* cDNA. S1 indicates the S1 RNA-binding domain. (**B**) Y2H assays showing the interaction between the truncated pTAC10s and subunits of PEP complex. The prey plasmid containing rpoA was used as a negative control for the interaction with pTAC10. DDO medium was used to validate yeast transformation and equal dropping.

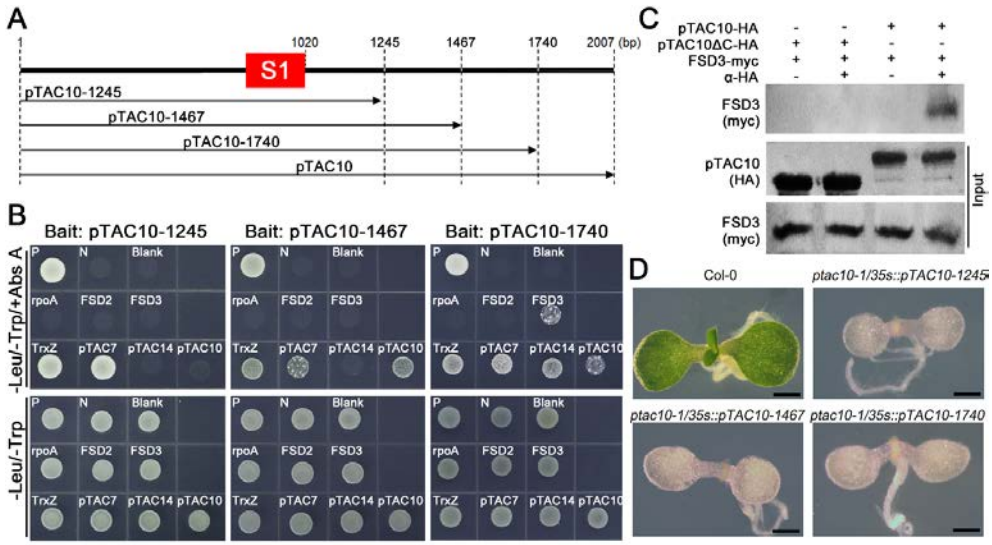
A
1
1020
1245
1467
1740
2007 (bp)
S1
pTAC10-1245
pTAC10-1467
pTAC10-1740
pTAC10
B
Bait: pTAC10-1245
Bait: pTAC10-1467
Bait: pTAC10-1740
-Leu/-Trp/+Abs A
-Leu/-Trp
P
N
Blank
rpoA
FSD2
FSD3
TrxZ
pTAC7
pTAC14
pTAC10
C
pTAC10-HA
pTAC10ΔC-HA
FSD3-myc
α-HA
FSD3 (myc)
pTAC10 (HA)
FSD3 (myc)
Input
D
Col-0
ptac10-1/35s::pTAC10-1245
ptac10-1/35s::pTAC10-1467
ptac10-1/35s::pTAC10-1740

Figure 10. pTAC10 C-terminal region downstream of the S1 domain is involved in the pTAC10-PAP interaction.

(**A**) Schematic showing a series of the truncated *pTAC10* structures. (**B**) Y2H assays using PAP prey plasmids and pTAC10-1245, pTAC10-1467, and pTAC10-1740 bait plasmids, respectively. (**C**) Co-IP analysis showing the pTAC10-FSD3 interaction. pTAC10-HA and pTAC10ΔC-HA indicate the full-length pTAC10 and pTAC10 without C-terminal region downstream of the S1 domain fused with HA epitope, respectively. FSD3-myc indicates intact FSD3 fused with myc epitope. (**D**) Complementation test of *ptac10-1* mutants using a series of C-terminal region-truncated *pTAC10*s depicted as (A). Scale bars = 1 mm.

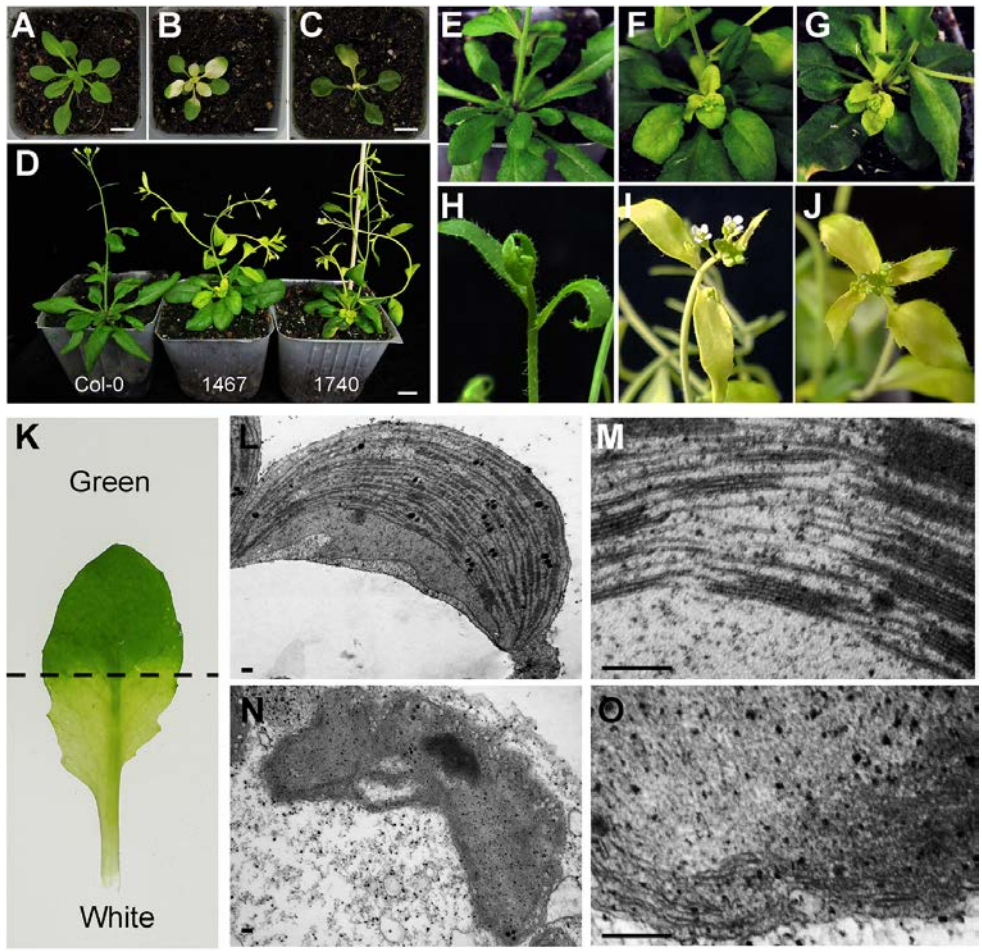
A
B
C
D
Col-0
1467
1740
E
F
G
H
I
J
K
Green
White
L
M
N
O

Figure 11. Overexpression of C-terminal truncated *pTAC10* in wild-type plants induces abnormal whitening phenotypes.

(**A-C**) Images showing 4-week-old Col-0 (A) and abnormal whitening-occurred *35s::pTAC10-1467* (B), and *35s::pTAC10-1740* (C) plants. Scale bar = 1 cm. (**D**) Seven-week-old *35s::pTAC10-1467* (1467) and *35s::pTAC10-1740* (1740) plants displayed the abnormal whitening phenotype. (**E-J**) High resolution images of Col-0 (E and H), *35s::pTAC10-1467* (F and J) and *35s::pTAC10-1740* (G and J) plants. (**K-O**) Image of an abnormally whitened leaf collected from *35s::pTAC10-1467* (K). The ultrastructures of plastids in the green part (L and M) and the white part (N and O) of this leaf were magnified for high-resolution display. Scale bar = 200 nm.

Supplementary Materials

Supplementary Table 1. Expression pattern of plastid genes in *ptac10-1* mutant.

Accession No	Gene	Fold change (*ptac10-1*/Col-0) (Down-regulation)
ATCG00430	photosystem II reaction center protein	0.073
ATCG00580	photosystem II reaction center protein	0.105
ATCG00680	photosystem II reaction center protein	0.224
ATCG00020	photosystem II reaction center protein	0.238
ATCG00070	photosystem II reaction center protein	0.333
ATCG00280	photosystem II reaction center protein	0.336
ATCG00630	subunit J of photosystem I	0.237
ATCG00490	large subunit of RUBISCO	0.348
ATCG00950	ribosomal RNA	0.110
ATCG01180	ribosomal RNA	0.110
ATCG01210	ribosomal RNA	0.129
ATCG00920	ribosomal RNA	0.129
ATCG00330	ribosomal protein S14	0.416
ATCG00420	NADH dehydrogenase subunit J	0.106
ATCG00440	NADH:ubiquinone/plastoquinone oxidoreductase	0.451
Accession No	**Gene**	**(Up-regulation)**
ATCG00190	Plastid-encoded RNA polymerase subsuit	2.990
ATCG00180	Plastid-encoded RNA polymerase subsuit	3.728
ATCG00170	Plastid-encoded RNA polymerase subsuit	4.327
ATCG00740	Plastid-encoded RNA polymerase subunit	6.018
ATCG00790	ribosomal protein L16	2.190
ATCG00820	ribosomal protein S19	2.444
ATCG00160	ribosomal protein S2	2.999
ATCG00650	ribosomal protein S18	3.021
ATCG00380	ribosomal protein S4	3.126

ATCG00810	ribosomal protein L22	3.251
ATCG01240	ribosomal protein S7	3.307
ATCG00900	ribosomal protein S7	3.325
ATCG00660	ribosomal protein L20	3.379
ATCG00780	ribosomal protein L14	3.737
ATCG00800	ribosomal protein S3	3.963
ATCG01230	ribosomal protein S12B	4.078
ATCG00905	ribosomal protein S12C	4.317
ATCG00770	ribosomal protein S8	4.822
ATCG00640	ribosomal protein L33	5.147
ATCG00750	ribosomal protein S11	6.334
ATCG00360	YCF3	4.503
ATCG00520	YCF4	4.278
ATCG01000	YCF1.1	8.293
ATCG01130	YCF1.2	12.53
ATCG01100	NADH dehydrogenase family protein	3.377
ATCG01010	NADH-Ubiquinone oxidoreductase	7.305
ATCG01110	NADH dehydrogenase subunit H	12.56
ATCG00670	plastid-encoded CLP P	5.960
ATCG01060	PsaC subunit of photosystem I.	8.101
ATCG00500	acetyl-CoA carboxylase carboxyl transferase subunit beta	11.366

Supplementary Table 2. Expression pattern of *PAPs* in *ptac10-1* mutant.

Accession No	Gene	Fold change (*ptac10-1*/Col-0)
AT5G51100	FSD2	1.979
AT5G23310	FSD3	2.255
AT3G06730	TrxZ	1.090
AT1G63680	MurE-like	2.215
AT3G54090	FLN1	1.434
AT1G74850	pTAC2	1.532
AT3G04260	pTAC3	2.412
AT1G21600	pTAC6	3.014
AT5G24314	pTAC7	1.306
AT3G48500	pTAC10	0.273
AT2G34640	pTAC12	2.089
AT4G20130	PTAC14	1.399

Supplementary Table 3. Primers used in this study.

Name	Sequence	Purpose
pTAC10 geno-5	CCCTTGTCATCTCTCCGTGT	*ptac10-1* genotype
pTAC10 geno-3	ACTGATTTTACCATCTCCGG	*ptac10-1* genotype
Vector Spe-5	CATAAGCTCTTTACAGGCGTG	*ptac10-1* genotype
pTAC10 bait-5	GCCATGGAGGCCGAATTCCCGATGCAGATTTGCCAAACCAAG	Yeast two hybrid
pTAC10 bait-3	CTGCAGGTCGACGGATCCCCTCAGTCTGTCAAGACTTGAG	Yeast two hybrid
pTAC10NS1 bait-3	CTGCAGGTCGACGGATCCCCGCGCAACTCCAAGGGAAAC	Yeast two hybrid
pTAC10N bait-3	CTGCAGGTCGACGGATCCCCAAAGGGAAGCTCATACATCCC	Yeast two hybrid
pTAC10S1 bait-5	GCCATGGAGGCCGAATTCCCGTACTATCCAGGGATGGTTTG	Yeast two hybrid
pTAC10C bait-5	GCCATGGAGGCCGAATTCCCGTTCGTCCATCCTAACATAG	Yeast two hybrid
pTAC10-1245 bait-3	CTGCAGGTCGACGGATCCCCTCAAATCATTTGCTCAGCTACATG	Yeast two hybrid
pTAC10-1467 bait-3	CTGCAGGTCGACGGATCCCCTCAAGCTTCCATCATTAGTTT	Yeast two hybrid
pTAC10-1740 bait-3	CTGCAGGTCGACGGATCCCCTCACTCTTGCTTGCTAATCTCTGAG	Yeast two hybrid
rpoA prey-5	GAGGCCAGTGAATTCCACCCGATGGTTCGAGAGAAAGTCAAAG	Yeast two hybrid
rpoA prey-3	TCCCGTATCGATGCCCACCCCTATTTTTTTTCTAGAATGTCT	Yeast two hybrid
rpoB prey-5	GAGGCCAGTGAATTCCACCCGATGCTTGGGGATGAAAAAGAG	Yeast two hybrid
rpoB prey-3	TCCCGTATCGATGCCCACCCTTAAACTTCCTTCCTATTAATC	Yeast two hybrid
FSD2 prey-5	GAGGCCAGTGAATTCCACCCGATGATGAATGTTGCAGTGAC	Yeast two hybrid
FSD2 prey-3	TCCCGTATCGATGCCCACCCTTAGTCAACCTCAGATACATC	Yeast two hybrid
FSD3 prey-5	GAGGCCAGTGAATTCCACCCGATGAGTTCTTGTGTTGTGAC	Yeast two hybrid

FSD3 prey-3	TCCCGTATCGATGCCCACCCTTAAGCG ATTGGGATGTTGG	Yeast two hybrid
TrxZ prey-5	GAGGCCAGTGAATTCCACCCGATGGCT CTTGTTCAATCCAG	Yeast two hybrid
TrxZ prey-3	TCCCGTATCGATGCCCACCCTCACATCT CGTTGTCAATGA	Yeast two hybrid
MurE prey-5	GAGGCCAGTGAATTCCACCCGATGGCG TTCACCTTTCTCTC	Yeast two hybrid
MurE prey-3	TCCCGTATCGATGCCCACCCTTAATGAC TCTCTGGTAACCG	Yeast two hybrid
pTAC2 prey-5	GAGGCCAGTGAATTCCACCCGATGAAC CTAGCAATTCCAAATC	Yeast two hybrid
pTAC2 prey-3	TCCCGTATCGATGCCCACCCTTAAGCT GTGCTCCCTGCTAG	Yeast two hybrid
pTAC6 prey-5	GAGGCCAGTGAATTCCACCCGATGGCG TCTTCCGCCGCTTC	Yeast two hybrid
pTAC6 prey-3	TCCCGTATCGATGCCCACCCCTAGAAC CAATTTGAGACACTG	Yeast two hybrid
pTAC7 prey-5	GAGGCCAGTGAATTCCACCCGATGGCT TCCTTCACCTGTTCT	Yeast two hybrid
pTAC7 prey-3	TCCCGTATCGATGCCCACCCTCAAGTG TAGTACTCCAACAA	Yeast two hybrid
pTAC10 prey-5	GAGGCCAGTGAATTCCACCCGATGCAG ATTTGCCAAACCAAG	Yeast two hybrid
pTAC10 prey-3	TCCCGTATCGATGCCCACCCTCAGTCT GTCAAGACTTGAG	Yeast two hybrid
pTAC12 prey-5	GAGGCCAGTGAATTCCACCCGATGGCG TCAATATCAACCAC	Yeast two hybrid
pTAC12 prey-3	TCCCGTATCGATGCCCACCCTTAAGGA TCAGTCTCCTCTTC	Yeast two hybrid
pTAC14 prey-5	GAGGCCAGTGAATTCCACCCGATGGCT TCTTCAGTCTCTCTTC	Yeast two hybrid
pTAC14 prey-3	TCCCGTATCGATGCCCACCCTCAATAG AGTAACCGTTCTTG	Yeast two hybrid
S3 prey-5	GAGGCCAGTGAATTCCACCCGATGGG ACAAAAAATAAATCCAC	Yeast two hybrid
S3 prey-3	TCCCGTATCGATGCCCACCCTTATTCTT CGTCTACGAATATC	Yeast two hybrid
L12-1 prey-5	GAGGCCAGTGAATTCCACCCGATGGCG TCGACGACTCTCTC	Yeast two hybrid

L12-1 prey-3	TCCCGTATCGATGCCCACCCTTAAGCAATGGAGACTTTAGCAC	Yeast two hybrid
L29 prey-5	GAGGCCAGTGAATTCCACCCGATGCTTAGTCTCTCAATCGC	Yeast two hybrid
L29 prey-3	TCCCGTATCGATGCCCACCCTCAAGCAGATTTAGCAGCTTC	Yeast two hybrid
EF-TU prey-5	GAGGCCAGTGAATTCCACCCGATGGCGATTTCGGCTCCAGC	Yeast two hybrid
EF-TU prey-3	TCCCGTATCGATGCCCACCCTCATTCGAGGATCGTCCCAATAA	Yeast two hybrid
pTAC10 E2C-5	GGAACCAATTCAGTCGACTGGATCCATGCAGATTTGCCAAACCAAG	Co-IP
pTAC10 E2C-3	CAGGCCTCCGCTTGCGGCCGCGTCTGTCAAGACTTGAGTAC	Co-IP
pTAC10C E2C-3	CAGGCCTCCGCTTGCGGCCGCAAAGGGAAGCTCATACATCCC	Co-IP
FSD3 E3C-5	GGAACCAATTCAGTCGACTGGATCCATGAGTTCTTGTGTTGTGACG	Co-IP
FSD3 E3C-3	TGCTCCATAGCTTGTGCGGCCGCAGCGATTGGGATGTTGG	Co-IP
pTAC10 BP-5	GGGGACAAGTTTGTACAAAAAAGCAGGCTCCATGCAGATTTGCCAAACC	OX and GST fusion
pTAC10 full BP-3	GGGGACCACTTTGTACAAGAAAGCTGGGTCTCAGTCTGTCAAGACTTG	OX and GST fusion
pTAC10-1245 BP-3	GGGGACCACTTTGTACAAGAAAGCTGGGTCTCAAATCATTTGCTCAGCTACATG	OX
pTAC10-1467 BP-3	GGGGACCACTTTGTACAAGAAAGCTGGGTCTCAAGCTTCCATCATTAGTTT	OX
pTAC10-1740 BP-3	GGGGACCACTTTGTACAAGAAAGCTGGGTCTCACTCTTGCTTGCTAATCTCTGAG	OX
pTAC10-Nterm-GA-5	GGTCGACTCTAGAGGATCCCCGGATGCAGATTTGCCAAACC	OX
pTAC10-Nterm-GA-3	GTGAATTCGAGCTCGGTACCCGCGCAACTCCAAGGGAAAC	OX
pTAC10-Cterm-GA-5	GGTCGACTCTAGAGGATCCCCGGTTCGTCCATCCTAACATAG	OX
pTAC10-Cterm-GA-3	GTGAATTCGAGCTCGGTACCCTCAGTCTGTCAAGACTTGAG	OX
pTAC7 BP-5	GGGGACAAGTTTGTACAAAAAAGCAGGCTCCATGGCTTCCTTCACCTGTTC	MBP fusion

pTAC7 BP-3	GGGGACCACTTTGTACAAGAAAGCTG GGTCAGTGTAGTACTCCAACAAATAGC C	MBP fusion
TrxZ BP-5	GGGGACAAGTTTGTACAAAAAAGCAG GCTCCATGGCTCTTGTTCAATCCAG	MBP fusion
TrxZ BP-3	GGGGACCACTTTGTACAAGAAAGCTG GGTCCATCTCGTTGTCAATGATATCG	MBP fusion
FSD3 BP-5	GGGGACAAGTTTGTACAAAAAAGCAG GCTCCATGAGTTCTTGTGTTGTG	MBP fusion
FSD3 BP-3	GGGGACCACTTTGTACAAGAAAGCTG GGTCTTAAGCGATTGGGATGTTG	MBP fusion
pTAC10-5	CTCCTGTGATTCCCATTGATG	qRT-PCR
pTAC10-3	GCTGATATCTCTGAGCAATGC	qRT-PCR
pTAC12-5	GATCCTTAAACCTGGTTTTCG	qRT-PCR
pTAC12-3	CCATATGATACAAATCACTTGC	qRT-PCR
pTAC14-5	GTGCTCACTCCCTTGAGCTAC	qRT-PCR
pTAC14-3	CTAATCAAACTCATTAAAGCAGC	qRT-PCR
FSD3-5	AGAACGACAGGGCTAAGTATA	qRT-PCR
FSD3-3	GCGATTGGGATGTTGGGTTC	qRT-PCR
TrxZ-5	CGCCGTAATTTAGGATTGG	qRT-PCR
TrxZ-3	CCGACCAGATCAACAGCTC	qRT-PCR
rpoB-5	GAACATCTGCAATACCCGG	qRT-PCR
rpoB-3	GTTCTACCAATTGATATGTTTCC	qRT-PCR
rbcL-5	GCTGCTGAATCTTCTACTGG	qRT-PCR
rbcL-3	GAGTTTCTTCTCCTGGAACG	qRT-PCR
psbA-5	GTCCTTGGATTGCTGTTGC	qRT-PCR
psbA-3	GAGATTCCTAGAGGCATACC	qRT-PCR
psaB-5	GAAGCGTTTACTCGAGGAGG	qRT-PCR
psaB-3	CCCTATTAAGGATAGGGCAG	qRT-PCR
psbD-5	GGATGAGTGCTCTTGGAGTAG	qRT-PCR
psbD-3	GTCTCAAATTCTGGATCTTC	qRT-PCR
AS1-5	GACGCAGAGGCCAAAGACCA	qRT-PCR
AS1-3	AACAAAGAGTTTAGGAGACGG	qRT-PCR
AS2-5	CTACGACGGTGGGATTCTTG	qRT-PCR
AS2-3	TCGACGAAGATGAACACCACC	qRT-PCR
KAN1-5	CAGGAGCAAAGGTCGAATGATC	qRT-PCR

KAN1-3	CAAGAAAGTCATTTCTCGTGCC	qRT-PCR
ARF3-5	GGGAATTCCATGAAAGGTGC	qRT-PCR
ARF3-3	CCAAAGAACCCTTCTAGAGAGC	qRT-PCR
YAB5-5	GCGAGTACCTTCTGCGTACA	qRT-PCR
YAB5-3	GTTACTCTCCAGCATTAGACC	qRT-PCR
ATC2-5	CTTGCACCAAGCAGCATGAA	qRT-PCR
ATC2-3	CCGATCCAGACACTGTACTTCC	qRT-PCR

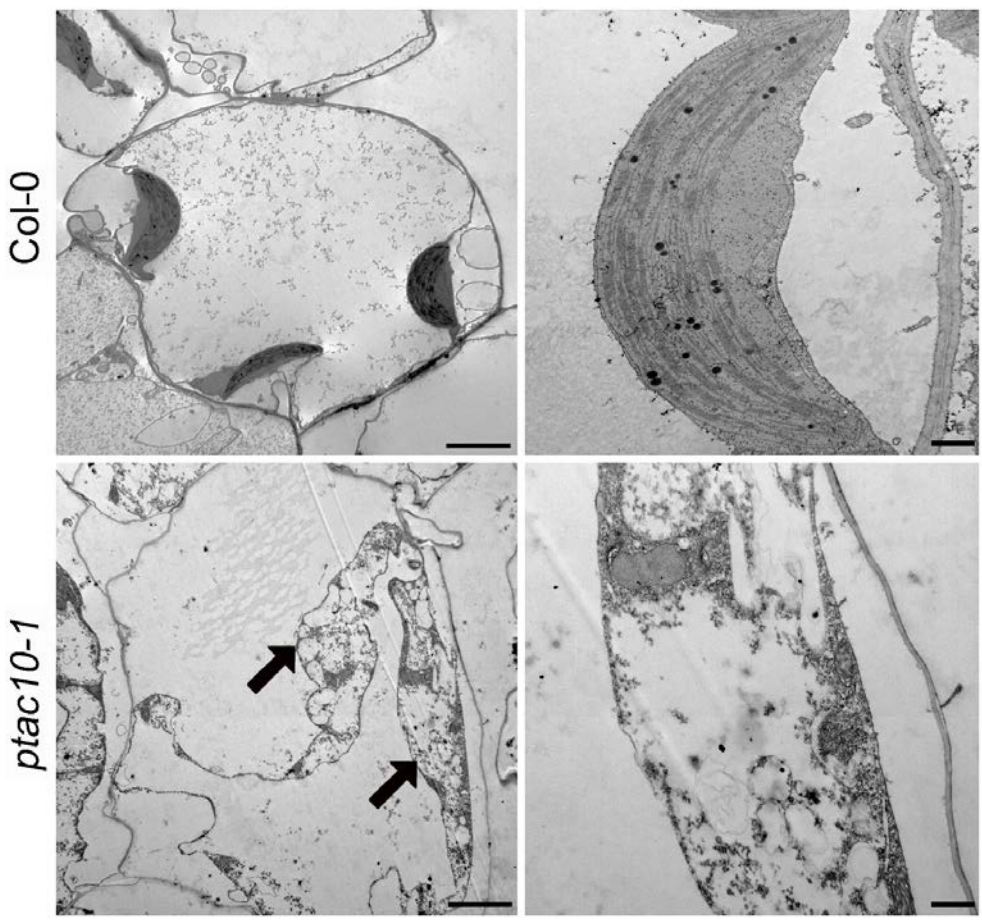
Col-0
ptac10-1

Supplementary Figure 1. Ultrastructure of plastids in *ptac10-1* mutants.

Ultrastructure of plastids in 1-week-old wild-type (top) and *ptac10-1* mutant (bottom) plants grown in half-strength MS medium. Plastid ultrastructure was observed by TEM. Black arrows indicate abnormally large plastids observed in mutants, which were not found in Col-0. Scale bars = 2 μm in left images and 500 nm in the right images.

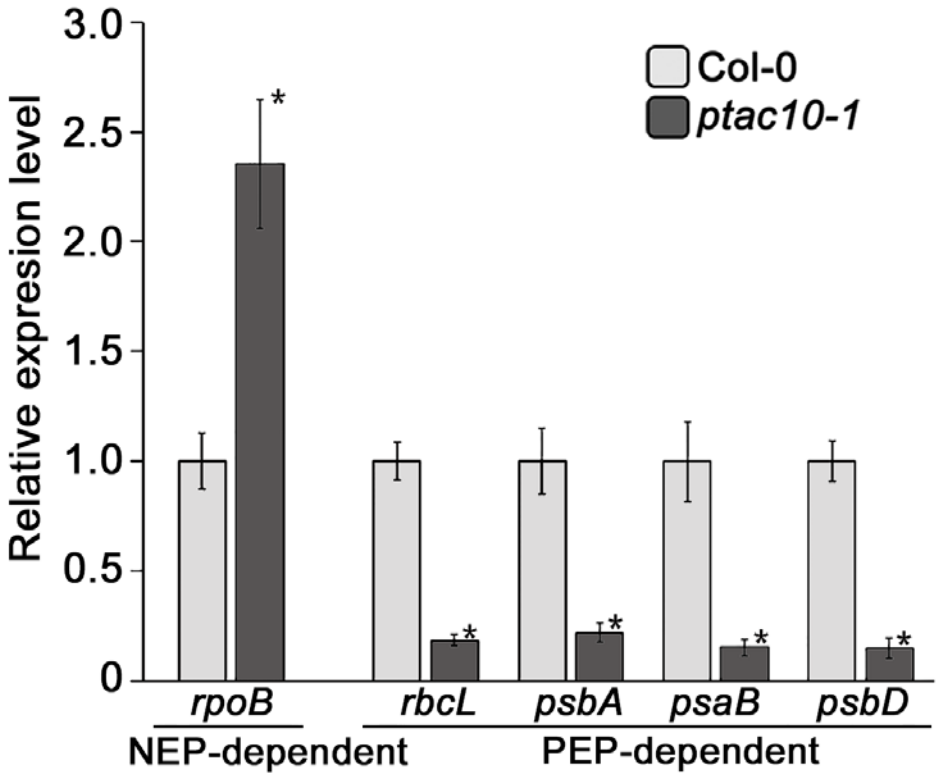
Relative expresion level
3.0
2.5
2.0
1.5
1.0
0.5
0
Col-0
ptac10-1
*
rpoB
rbcL
psbA
psaB
psbD
NEP-dependent
PEP-dependent

Supplementary Figure 2. Analysis of expression levels of plastid genes in *ptac10-1* mutants.

Expression levels of NEP- or PEP-dependent genes were analyzed by qRT-PCR. Total RNA was extracted from 7-day-old Col-0 and *ptac10-1* mutant seedlings, respectively. Error bars indicate SD. The asterisks indicated significant difference between *ptac10-1* and Col-0 (p-value < 0.01, t-test).

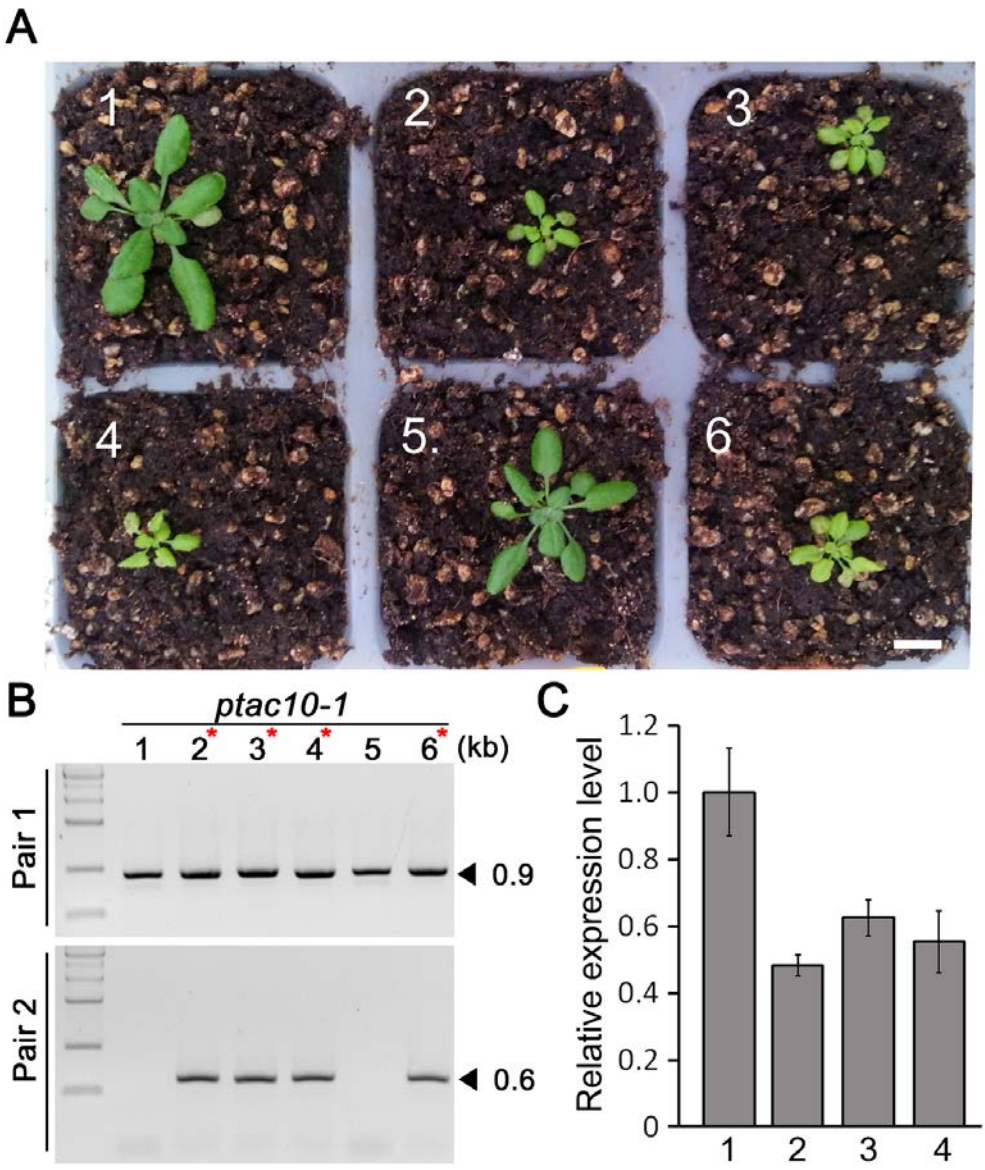
A
1
2
3
4
5.
6
B
ptac10-1
1 2* 3* 4* 5 6* (kb)
Pair 1
0.9
Pair 2
0.6
C
Relative expression level
1.2
1.0
0.8
0.6
0.4
0.2
0
1 2 3 4

Supplementary Figure 3. Expression level of *pTAC10* in heterozygous *ptac10-1* mutants.

(**A**) Image showing the survived green progeny of the self-pollinated heterozygous *ptac10-1* mutants grown in soil for 4 weeks. Scale bar = 1 cm. (**B**) Genotyping results of the indicated individual plants in (A). Red asterisks indicated heterozygous *ptac10-1* mutants (+/-) and the others are homozygous wild-types (+/+). (**C**) Expression level of *pTAC10* in these plants. Error bars indicate SD.

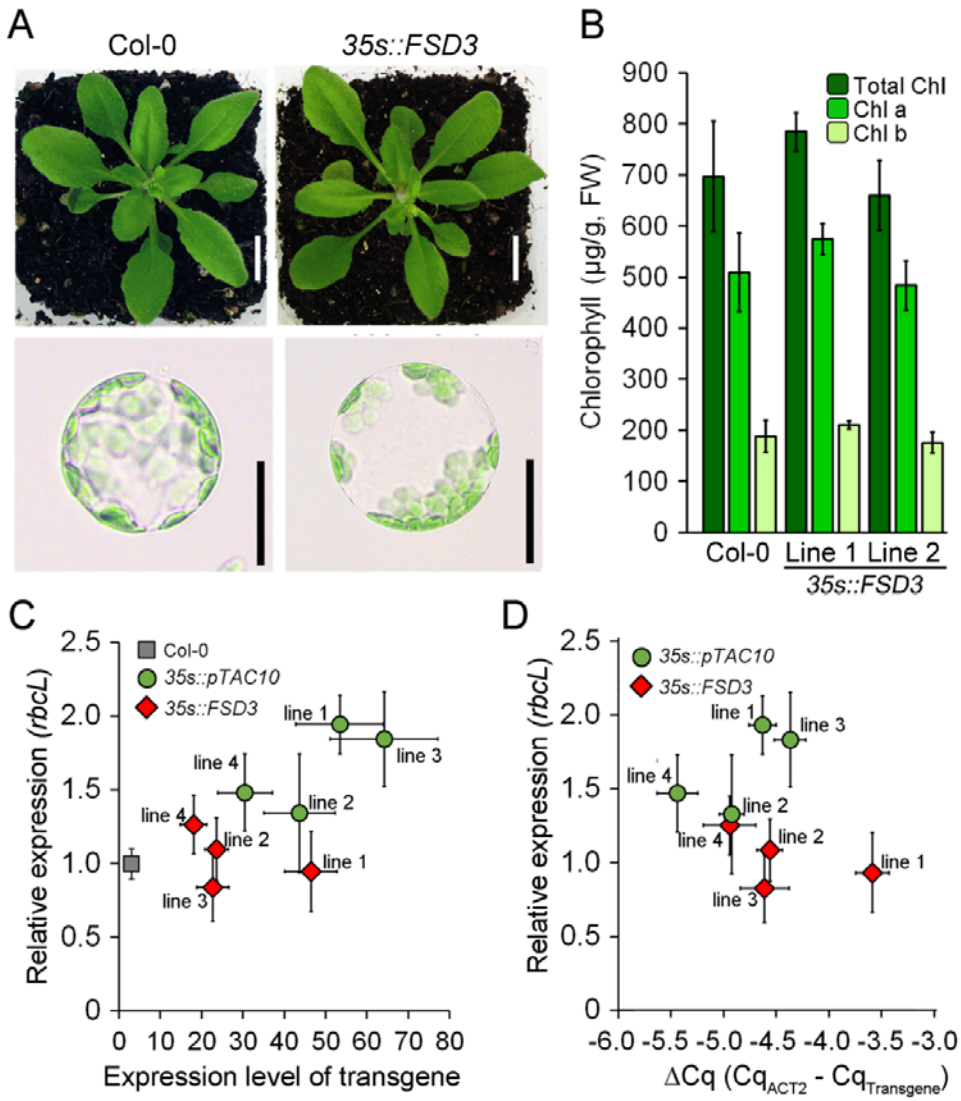
A
Col-0
35s::FSD3
B
Total Chl
Chl a
Chl b
Chlorophyll (µg/g, FW)
900
800
700
600
500
400
300
200
100
0
Col-0
Line 1
Line 2
35s::FSD3
C
Col-0
35s::pTAC10
35s::FSD3
Relative expression (rbcL)
2.5
2.0
1.5
1.0
0.5
0
line 1
line 2
line 3
line 4
0 10 20 30 40 50 60 70 80
Expression level of transgene
D
35s::pTAC10
35s::FSD3
Relative expression (rbcL)
-6.0 -5.5 -5.0 -4.5 -4.0 -3.5 -3.0
ΔCq (Cq ACT2 - Cq Transgene)

Supplementary Figure 4. Overexpression of *FSD3* does not induce the unique phenotypes observed in *pTAC10*-overexpressing plants.

(**A**) Morphology of Col-0 and *35s::FSD3* plants grown in soil for 5 weeks (top) and protoplasts isolated from these plants (bottom). Scale bar = 1 cm in top images and 10 μm in bottom images. (**B**) Quantification of chlorophyll contents in wild-type (Col-0) and two independent lines of *35s::FSD3* (line 1 and 2). (**C** and **D**) Scatter plots displaying varied expression levels of a transgene, *pTAC10* or *FSD3,* with the standard of Col-0 (C), and the abundance of the transgene transcripts (D) in these transgene-overexpressing plants.

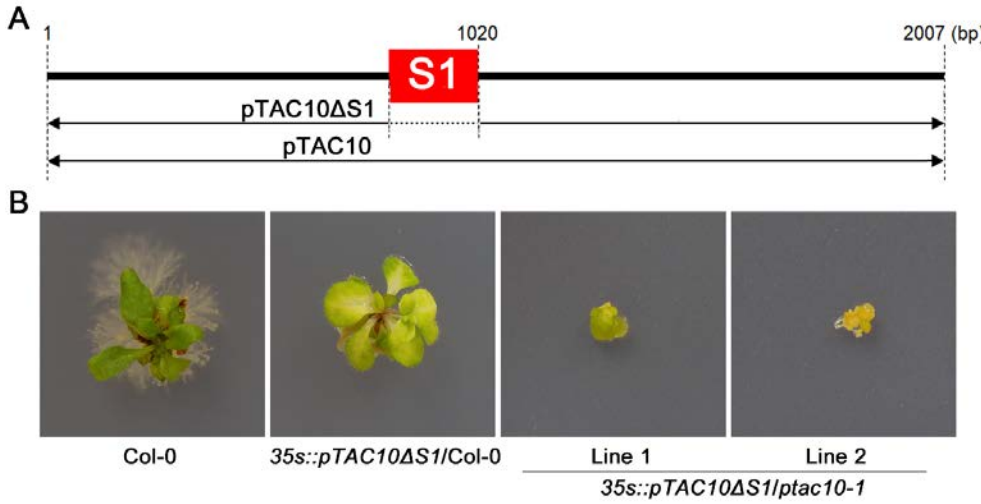
A
1
1020
2007 (bp)
S1
pTAC10ΔS1
pTAC10
B
Col-0
35s::pTAC10ΔS1/Col-0
Line 1
Line 2
35s::pTAC10ΔS1/ptac10-1

Supplementary Figure 5. Introduction of *pTAC10* without the S1 domain into *ptac10-1* did not rescue the mutant phenotype.

(**A**) Schematic of *pTAC10* lacking the S1 domain (pTAC10ΔS1). (**B**) Root-derived calli from Col-0 and *ptac10-1* mutants transformed with 35s::pTAC10ΔS1 plasmid and tissue regeneration was progressed.

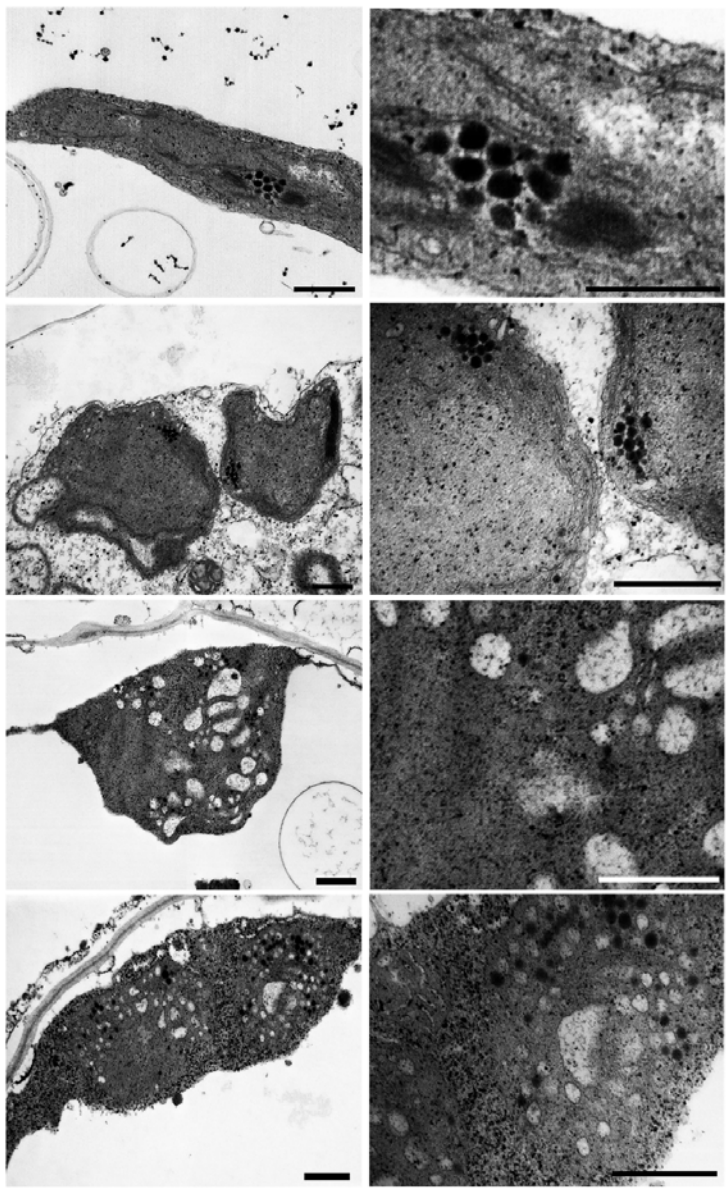

Supplementary Figure 6. Ultrastructure of plastids in the whitened leaves of plants overexpressing *pTAC10-1467*.

Ultrastructure of plastids in the abnormally whitened leaves of *35s::pTAC10-1467* transgenic plants were observed by TEM (left) and at a higher magnification (right). Scale bars = 500 nm.

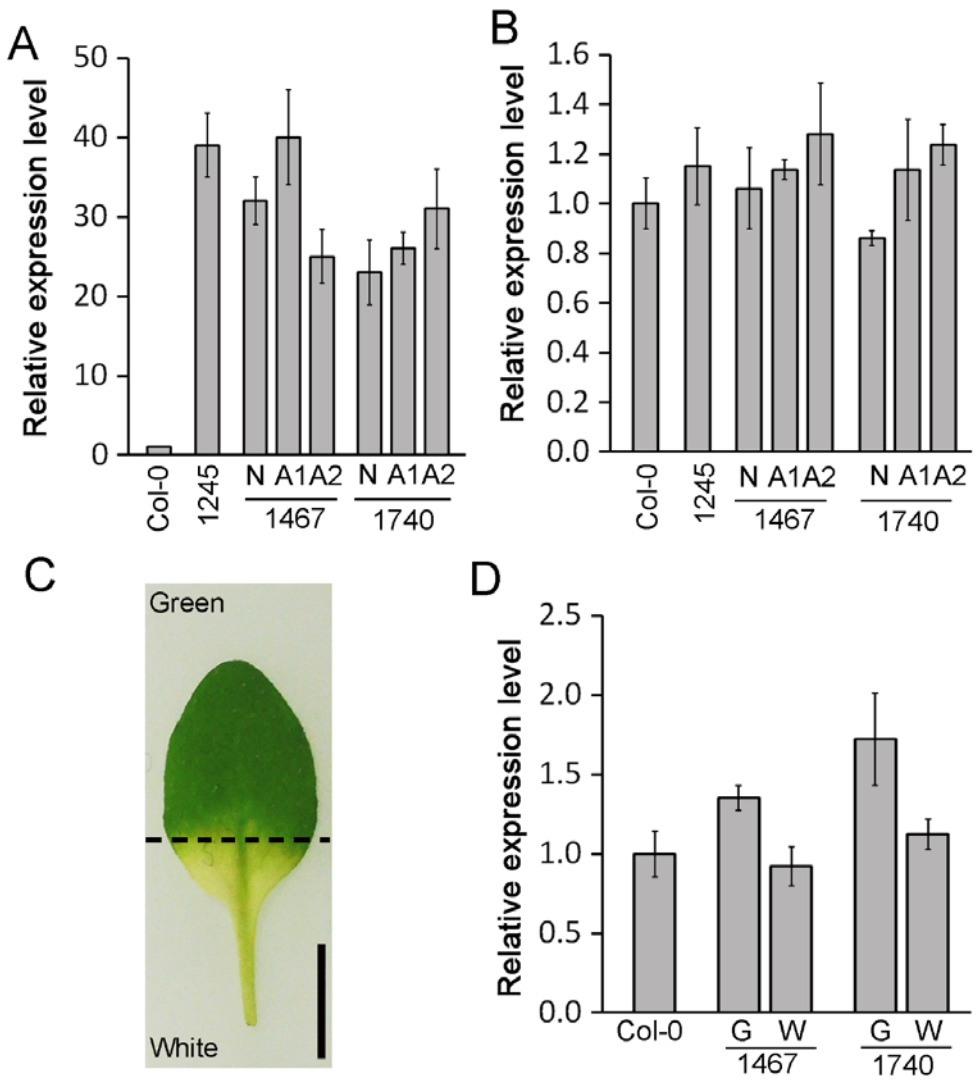
A
Relative expression level
50
40
30
20
10
0
Col-0
1245
N A1A2
1467
N A1A2
1740
B
Relative expression level
1.6
1.4
1.2
1.0
0.8
0.6
0.4
0.2
0.0
Col-0
1245
N A1A2
1467
N A1A2
1740
C
Green
White
D
Relative expression level
2.5
2.0
1.5
1.0
0.5
0.0
Col-0
G W
1467
G W
1740

Supplementary Figure 7. Expression analysis of the truncated transgenes and endogenous *pTAC10* in the C-terminal truncated *pTAC10*-overexpressing plants.

(**A**) Expression level of the transgenes in the indicated C-terminal truncated *pTAC10*-overexpressing plant lines. (**B**) Expression level of endogenous *pTAC10* in the indicated transgenic plants. 1245, 1467, and 1740 indicate *35s::pTAC10-1245*, *35s::pTAC10-1467*, and *35s::pTAC10-1740* transgenic plants. N, A1, and A2 indicate the independent transgenic lines displaying the normal green phenotype (N), and the abnormal whitening phenotype (A1 and A2), respectively. (**C**) Image of a leaf collected from *35s::pTAC10-1467* plant, which showed abnormal whitening phenotype. (**D**) qRT-PCR results showing expression levels of endogenous *pTAC10* in the green and whitened parts of leaves with abnormal whitening phenotypes. The leaves were collected from *35s::pTAC10-1467* transgenic plants. G and W indicate green and white parts of the leaves. Error bars indicate SD. Scale bar = 0.5 cm.

요약(국문 초록)

색소체 유래 RNA 중합효소 (Plastid-encoded RNA polymerase, PEP) 는 색소체 유전자의 발현을 조절하는 중요한 기능을 하는 효소로 엽록체 발달에 반드시 필요하다. 여러 사전 연구에 의해 PEP 의 활성은 색소체에서 유래한 PEP 코어 단백질과 핵에서 유래한 PEP 보조 단백질 (PEP-associated proteins, PAPs) 이 얼마나 성공적으로 모여 PEP 복합체를 구성하는가에 의해 결정된다는 것이 알려졌다. 또한 최근 연구에서 PEP-PAP 또는 PAP-PAP 상호작용과 같은 PEP 복합체를 구성하는 여러 단백질 간의 광범위한 상호 작용이 기능성 PEP 복합체를 구성하는데 중추적인 역할을 한다는 것이 보고된 바 있다. 이 연구에서는 유묘 시기 백화현상이 일어나 성장이 중단되어 죽는 표현형을 가진 *ptac10-1* 돌연변이체를 발견하였다. 이 돌연변이체는 S1 RNA 결합 도메인을 포함하는 PEP 보조 단백질 3 (PEP-associated protein 3, pTAC10/PAP3) 을 암호화하는 유전자의 발현이 억제되어 있었으며, 측면염기서열분석법 (FSTs) 과 유전학적 보완 검사 등을 통해 *pTAC10* 유전자가 이 돌연변이 표현형의 원인임을 밝혀내었다. *ptac10-1* 돌연변이와 *pTAC10* 과발현 식물을 이용한 유전자 발현 분석 실험은 *pTAC10* 유전자의 발현 수준과 엽록체 발달 수준 사이의 상관관계를 보여주었다. 또한 pTAC10 과 PEP 복합체의 구성 단백질 간의 상호작용을 분석한 결과, pTAC10 은 FSD2, FSD3, pTAC7, pTAC14, TrxZ 및 pTAC10 자신을 포함한 여러 PAP 단백질과 상호작용하지만 rpoA 또는 rpoB 와 같은 PEP 코어 단백질과는 상호작용하지 않는다는 것이 밝혀졌다. 더욱이 다양하게 절단된 pTAC10 을 이용한 단백질 상호작용 분석은

pTAC10 의 S1 도메인이 pTAC10 의 기능에 필수적이지만 pTAC10 과 PAP 간의 상호작용에는 관여하지 않는다는 것을 보여주었다. 오히려 다른 PAP 과의 상호작용은 S1 도메인을 기준으로 C 말단 방향에 위치한 영역이 담당한다는 것이 밝혀졌다. 또한 C 말단이 다양하게 절단된 *pTAC10* 을 야생형 식물에서 과발현시켰을 때, 야생형에서는 발견되지 않는 비정상적인 백화현상이 유도되는 현상을 관찰하였다. 이는 불완전한 pTAC10 으로 인해 완전한 PEP 복합체의 완성이 방해 받으면 엽록체의 발달이 저해됨을 시사한다. 이러한 연구 결과는 pTAC10 이 다른 여러 PAP 과 상호작용을 통해 엽록체의 발달에 중요한 PEP 복합체를 구성하는 필수 요소임을 보여주었다.

주요어 : 엽록체, 엽록체 발달, 엽록체 유래 RNA 중합효소, 엽록체 유래 RNA 중합효소 보조 단백질, `pTAC10/PAP3

학 번 : 2015-23143